# The coordination chemistry of nitrosyl in cyanoferrates. An exhibit of bioinorganic relevant reactions

**José A. Olabe**
*Department of Inorganic, Analytical and Physical Chemistry and INQUIMAE, CONICET, Facultad de Ciencias Exactas y Naturales, Universidad de Buenos Aires, Pabellón 2, Ciudad Universitaria, C1428EHA, Buenos Aires, Argentina*

Sodium nitroprusside (SNP, $Na_2[Fe(CN)_5NO].2H_2O$) is a widely used NO-donor hypotensive agent, containing the formally described nitrosonium ($NO^+$) ligand, which may be redox interconverted to the corresponding one-electron ($NO^\bullet$) and two-electron ($NO^-$/HNO) reduced bound species. Thus, the chemistry of the three nitrosyl ligands may be explored with adequate, biologically relevant substrates. The nitrosonium complex, $[Fe(CN)_5NO]^{2-}$, is formed through a reductive nitrosylation reaction of $[Fe^{III}(CN)_5H_2O]^{2-}$ with NO, or, alternatively, through the coordination of $NO_2^-$ into $[Fe^{II}(CN)_5H_2O]^{3-}$ and further proton-assisted dehydration. It is extremely inert toward $NO^+$-dissociation, and behaves as an electrophile toward different bases: $OH^-$, amines, thiolates, etc. Also, SNP releases NO upon UV-vis photo-activation, with formation of $[Fe^{III}(CN)_5H_2O]^{2-}$. The more electron rich $[Fe(CN)_5NO]^{3-}$ may be prepared from $[Fe^{II}(CN)_5H_2O]^{3-}$ and NO, and is also highly inert toward the dissociation of NO ($k = 1.6 \times 10^{-5}$ $s^{-1}$, 25.0 ºC, pH 10.2). It reacts with $O_2$ leading to SNP, with the intermediacy of a peroxynitrite adduct. The $[Fe(CN)_5NO]^{3-}$ ion is labile toward the release of *trans*-cyanide, forming the $[Fe(CN)_4NO]^{2-}$ ion. Both complexes exist in a pH-dependent equilibrium, and decompose thermally in the hours-time scale, releasing cyanides and NO. The latter may further bind to $[Fe(CN)_4NO]^{2-}$ with formation of a singlet dinitrosyl species, $[Fe(CN)_4(NO)_2]^{2-}$, which in turn is unstable toward disproportionation into SNP and $N_2O$, and toward the parallel formation of a tetrahedral paramagnetic dinitrosyl compound, $[Fe(CN)_2(NO)_2]$. Emerging studies with the putative nitroxyl complex, $[Fe(CN)_5HNO]^{3-}$, should allow for a complete picture of the three nitrosyl ligands in the same pentacyano-fragment. The present Perspective, based on an adequate characterization of structural and spectroscopic properties, will focus on the kinetic and mechanistic description of the above mentioned reactions, which display a versatile scenario, fundamentally related to the biologically relevant processes associated with NO-reactivity.

## Introduction

Sodium nitroprusside (SNP, $Na_2[Fe(CN)_5NO].2H_2O$) was characterized in the middle of the 19th century,[1] and its blood-pressure lowering ability has been known since 1929.[2] Its clinical use as an hypotensive agent spans more than four decades,[3] though only recently has its pharmacological effect been attributed to its NO-donor ability. Much later in the 1980s, the endothelium derived relaxing factor (EDRF) was identified as NO, and its biosynthesis in mammals from L-arginine mediated by the enzyme NO synthase was discovered, together with the recognition of diverse physiological roles for NO, comprising blood pressure control, neurotransmission and immune response, tissue damage and carcinogenesis, as well as in the onset of disease states involving NO imbalances.[4-6] An enormous effort is being directed to studies on the chemistry and biochemistry of NO. As the principal targets of NO under bioregulatory conditions are metal centers, primarily iron proteins, a specific goal is devoted to the chemistry of metallonitrosyls.[7]

Despite the complex nature and intrinsic difficulties for the mechanistic elucidation of the *in vivo* processes associated with NO biochemistry, it is currently accepted that basic coordination chemistry remains behind the scene.[8] Thus, a model biomimetic approach justifies the interest in structure and reactivity studies of NO with metalloporphyrins,[9-12] or with classical complexes such as the cyanometallates.[12,13] In this context, a consistent characterization of the metal-NO interaction is needed, based on structural and spectroscopic grounds, as well as on the main reactivity modes dealing with the formation/dissociation of the bonds and with the redox reactions toward biologically relevant substrates: oxygen and related oxidants, thiolates, amines, etc.

The pentacyanoferrate-fragments constitute a valuable platform for these studies. The aqua-derivatives, $[Fe^{II,III}(CN)_5H_2O]^{3,2-}$, are accessible precursors for the synthesis of variable $[Fe^{II,III}(CN)_5L]^{n,(n-1)-}$ complexes, with L = $NH_3$, amines, $NO_2^-$, CO, py, etc.[14] Certainly, the nitrosyl ligands in different redox states: $NO^+$ (nitrosonium), $NO^\bullet$ and $NO^-$ (nitroxyl), are qualified members of this series, and their chemistry constitute the main subject of the present Perspective. We rely on previous reviews on the structure[15] and reactivity[12,16-20] of metal nitrosyls, some of them devoted

specifically to SNP.[12,19,20] The present critical discussion will focus on our results obtained mainly over the past six years with the cyano-nitrosyl complexes. The versatile scenario of reaction types relevant to NO-chemistry and biochemistry will be highlighted, namely ligand interchange, linkage isomerizations related to photo-processes, reductive nitrosylations, *trans*-labilizations, nucleophilic and electrophilic additions, autoxidations, dinitrosylations and disproportionations, etc. The detailed mechanisms of some of these reactions are amenable to a deeper insight and constitute a stimulating area of research, relevant to the proper understanding of the nitrogen cycles in Nature. An attempt will be made to better illustrate this Perspective by extending the approach to some related $[MX_5NO]^x$ complexes, with adequate consideration of the influence of the coligands X on the electronic structure and reactivity.

## Electronic structure of metal nitrosyls

Transition metal nitrosyl complexes span variable geometries, coordination numbers and electronic properties due to the differences in electronic configurations of the metal centers and *covalent* MNO interactions.[8,15] Focusing on pseudo-octahedral $[MX_5NO]^x$ complexes, we describe them as $\{MNO\}^n$, with $n$ standing for the number of electrons in the metal $d$ and $\pi^*_{NO}$ orbitals.[15c] Although not explicitly included in this fragment-formalism, the X-coligands indeed influence the detailed electronic density on each of the MNO atoms. This influence may be considered a perturbation ("fine-tuning") on the structural and reactivity properties, mainly determined by the functional group MNO and particularly by $n$, which attains values of 6, 7, 8 for most of the examples considered in this Perspective. Given the emphasis on the covalent nature of the M-N-O bonds, the use of limiting descriptions with metal oxidation-states and charges at the nitrosyl ligands could be severely questioned. As discussed below, this practice becomes useful when the available spectroscopic and/or theoretical tools enable to sustain such an electronic distribution, at least as a limiting case, and has been used for describing the reactivity of nitrosyl in a biorelevant scenario.[21] Table 1 displays a summary of structural and spectroscopic indicators for characteristic nitrosyl complexes with $n$ = 6, 7 and 8.[22-24] The $\{MNO\}^n$ systems may act as electron reservoirs, with the electrons susceptible to be promptly added or removed by chemical or electrochemical means.[17]

**a) $n$ = 6**

The more commonly found nitrosyl compounds pertain to the $\{MNO\}^6$ class. All are diamagnetic and display comparatively high stretching NO-frequencies, $\nu_{NO}$, most of them in the range 1800-2000 $cm^{-1}$, depending on the donor-acceptor abilities of the $MX_5$ fragments.[22] The M-N and N-O distances indicate a multiple bond order in the *systematically linear* MNO moieties, with a few exceptions for complexes containing strongly $\sigma$-donor *trans*-coligands.[10] The detailed electronic structure in the $\{MNO\}^6$ moieties comprises $M^{II}NO^+$ as the dominant contribution (for the group 8 metals), on the basis of the magnetic, IR and UV-vis spectral results and theoretical calculations. Mössbauer spectroscopy supports this description for iron complexes displaying small isomer shifts (*ca.* 0 mm $s^{-1}$) and large quadrupole splitting parameters.[22a-e,23e] The "normal" $Ir^{III}NO^+$ distribution also holds for the alkaline salts of the $[IrCl_5NO]^-$ ion (Table 1),[22j] although singlet $Ir^{IV}NO^\bullet$ has been claimed for $PPh_4[IrCl_5NO]$, on the basis of XANES spectroscopy and solid-state DFT calculations.[22k]

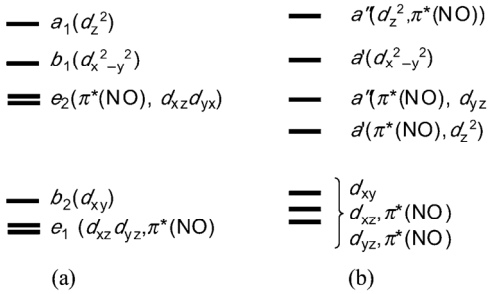


**Figure 1.** Simplified molecular orbital (MO) diagram for pseudooctahedral nitrosyl complexes containing $NO^+$, $NO^\bullet$ or $NO^-$ ligands ($n$ = 6, 7, 8, respectively)

Most of the nitrosonium complexes contain the $NO^+$ ligand ($S$ = 0) interacting with a low-spin $d^6$ metal center ($S$ = 0). This extreme ionic approach may be improved by allowing for $\sigma$- and $\pi$-contributions in the MNO moiety, influenced by X.[15-17] Thus, $NO^+$ is considered a weak $\sigma$-donor and very strong $\pi$-acceptor ligand. The nature of the $MX_5$ fragments may strongly influence $\nu_{NO}$, which decreases significantly if a strong $\pi$-donor metal is present (*viz.*, $Os^{II}$ or $Mn^I$ in Table 1). Figure 1a presents a simplified bonding model for $n$ = 6.[25] The six electrons are located in strongly bonding or nearly non-bonding, predominantly metal orbitals, with a vacant antibonding degenerate LUMO, primarily of $\pi^*_{NO}$ character. The pioneering work with SNP allowed for assignments of the electronic transitions (*d-d* and MLCT) in the UV-vis spectra.[26]

Regarding reactivity, the strong M-N bonds are extremely inert toward the *thermal* release of the nitrosyl ligand, as for SNP and related complexes.[18-20] Strikingly, NO is released very fast (range 1-$10^4$ $s^{-1}$) from the "ferri-hemes",[16,27] and this has been tentatively traced to a contribution of the $Fe^{III}NO^\bullet$ limiting structure. NO and $[Fe^{III}(CN)_5H_2O]^{2-}$ are produced by irradiation of SNP in the UV-vis region.[28] This seems to be a general property of the $n$ = 6 systems, involving a formal metal oxidation and $NO^+$-reduction.[29] The photoreactivity arises as a consequence of weakening the M-N bond upon excitation, as predicted by the MO scheme in Fig. 1a. This property of $NO^+$ also manifests in the generalized electrophilic reactivity for the members of the $\{MNO\}^6$ series (see below).[18]

SNP was the first complex for which the presence of linkage isomers has been detected upon low-temperature laser irradiation of solid samples, with initial Mössbauer characterization.[30,31] The conversion of the *N*-bound NO to the end-on, linear $\eta^1$-ON (isonitrosyl), and to the side-on $\eta^2$-NO diamagnetic complexes has been demonstrated by using photo-crystallographic techniques,[22e,31] with additional characterization coming from differential scanning

**Table 1.** Total spin-state ($S$), nitrosyl stretching frequencies, $\nu_{NO}$, relevant distances, $d_{M\text{-}N}$, $d_{N\text{-}O}$, and angles, $\angle_{MNO}$, for selected nitrosyl complexes, $[MX_5NO]^x$, ordered according to the $\{MNO\}^n$ description (see text)

| | Compound | $S$ | $\nu_{NO}$ ($cm^{-1}$) | $d_{M\text{-}N}$ (Å) | $d_{N\text{-}O}$ (Å) | $\angle_{MNO}$ (deg) | Ref. |
|---|---|---|---|---|---|---|---|
| $n = 6$ | $[Fe(cyclam\text{-}ac)NO](PF_6)_2$ | 0 | 1904 | 1.663(4) | 1.132(5) | 175.5(3) | 22a |
| | $[Fe(`pyS_4')NO]PF_6$ | 0 | 1893 | 1.634(3) | 1.141(3) | 179.5(3) | 22b |
| | $[Fe(PaPy_3)NO](ClO_4)_2$ | 0 | 1919 | 1.677(2) | 1.139(3) | 173.1(2) | 22c |
| | $[Fe(TpivPP)(NO_2)NO]$ | 0 | 1893 | 1.668(2) | 1.132(3) | 180.0 | 22d |
| | $Na_2\ [Fe(CN)_5NO].2H_2O$ | 0 | 1945 | 1.6656(7) | 1.1331(10) | 176.03(7) | 22e |
| | $Na_2[Ru(CN)_5NO].2H_2O$ | 0 | 1926 | 1.776(3) | 1.127(6) | 173.9(5) | 22f |
| | $Na_2[Os(CN)_5NO].2H_2O$ | 0 | 1897 | 1.774(8) | 1.14(1) | 175.5(7) | 22g |
| | $K_3[Mn(CN)_5NO]$ | 0 | 1725 | 1.66(1) | 1.21(2) | 174(1) | 22h |
| | $(PPh_4)_2[OsCl_5NO]$ | 0 | 1802 | 1.830(5) | 1.147(4) | 178.5(8) | 22i |
| | $K[IrCl_5NO]$ | 0 | 1952 | 1.780(11) | 1.124(17) | 174.3(11) | 22j |
| $n = 7$ | $[Fe(cyclam\text{-}ac)NO](PF_6)$ | 1/2 | 1615 | 1.722(4) | 1.166(6) | 148.7(4) | 22a |
| | $[Fe(`pyS_4')NO]$ | 1/2 | 1648 | 1.712(3) | 1.211(7) | 143.8(5) | 22b |
| | $[Fe(PaPy_3)NO](ClO_4)$ | 1/2 | 1613 | 1.7515(16) | 1.190(2) | 141.29(15) | 22c |
| | $K(222)[Fe(TpivPP)(NO_2)NO]$ | 1/2 | 1668 | 1.840(6) | 1.134(8) | 137.4(6) | 23a |
| | $Na_3[Fe(CN)_5NO].2NH_3$ [a] | 1/2 | 1608 | 1.737 | 1.162 | 146.6 | 23b,24a |
| | $[Fe(Me_3TACN)(N_3)_2NO]$ | 3/2 | 1690 | 1.738(5) | 1.142(7) | 155.5(10) | 23c,d |
| | $[Fe(L^{pr})(NO)]$ [b] | 1/2,3/2 | 1682 | 1.749(2) | 1.182(3) | 147.0(2) | 23e |
| $n = 8$ | $[Fe(CN)_5HNO]^{3-}$ [a] | 0 | 1338 | 1.783 | 1.249 | 137.5 | 24a |
| | $[CoCl(en)_2NO](ClO_4)$ | 0 | 1611 | 1.820(11) | 1.043(7) | 124.4(11) | 24b |
| | $[Ru(`py^{bu}S_4')HNO]$ | 0 | 1358 | 1.875(7) | 1.242(9) | 130.0(6) | 24c |
| | $[OsCl_2(CO)(PPh_3)_2HNO]$ | 0 | 1410 | 1.915(6) | 1.193(7) | 136.9(6) | 24d |
| | $[IrHCl_2(PPh_3)_2HNO]$ | 0 | 1493 | 1.879(7) | 1.235(11) | 129.8(7) | 24e |

[a] Distances and angles for the anions are theoretically predicted values (DFT). [b] The solid contains *ca.* 50% of each isomer.

Abbreviations used for the ligands: cyclam-ac = monoanion of 1,4,8,11-tetraazacyclotetradecane-1-acetic acid; '$pyS_4$' = dianion of 2,6-bis(2-mercaptophenylthiomethyl)pyridine; $PaPy_3$ = monoanion of *N*,*N*-bis(2-pyridylmethyl)amine-*N*-ethyl-2-pyridine-2-carboxamide; TpivPP = dianion of α, α, α, α, -tetrakis(*o*-pivalamidophenyl)-porphyrin; $Me_3TACN$ = *N*,*N*′,*N*′′-trimethyl-1,4,7-triazacyclononane; $L^{pr}$ = dianion of 1-isopropyl-4,7-(4-*tert*-butyl-2mercaptobenzyl)-1,4,7-triazacyclononane; '$py^{bu}S_4$' = dianion of 2,6-bis(2-mercapto-3,5-di-*tert*-butylphenylthio)dimethylpyridine; $PPh_3$ = triphenylphosphine.

calorimetry,[30a] polarized UV-vis absorption[330a], IR-Raman[32] and Mössbauer spectroscopies.[30b] The isomers have been described as "metastable" states $MS_1$ and $MS_2$, originated in the thermal decay of an electronically excited state (ES) to the original ground state (GS), at 195 K and 151 K, respectively. Theoretical calculations suggest that both isomers lie in local minima on the GS potential energy surfaces, rejecting the alternative description as long-lived ES. Correlation diagrams have been calculated for SNP undergoing the deformation from $\eta^1$-NO (GS), through side-on $\eta^2$-NO ($MS_2$), to $\eta^1$-ON ($MS_1$).[33] These linkage isomerizations are likely processes occurring during the photochemistry of NO-release, as well as in related NO-transfer reactions.[15a] Recently, irradiation of single crystals *and aqueous solutions* of SNP at *room temperature* have been measured by transient absorption spectroscopy.[34] The build up of $MS_2$ from the ES was faster than 1 ns, and its monoexponential thermal decay was observed in *ca.* $10^{-7}$ s. Analogous linkage isomers have been discovered for $[Ru(CN)_5NO]^{2-}$ and $[Os(CN)_5NO]^{2-}$,[35] as well as for other members of the $\{M^{II}NO^+\}^6$ class.[30,31] The photoswitchable processes involving changes of the magnetic and/or optical properties to long lived metastable states could be relevant to energy and information storage, with possible photonic and biological applications.[30,31]

**b) $n = 7$**

By adding one electron to the complexes of the $\{MNO\}^6$ class, a new series of $\{MNO\}^7$ complexes can be obtained.[15,17] The available crystal structures allow for establishing well defined trends, complemented by IR, EPR and theoretical calculations. Table 1 includes some representative complexes, showing the bending of the MNO angle to *ca.* 140º, and the relative lengthening of the M-N and N-O bonds upon reduction. Figure 1b displays the new MO description under the lower symmetry conditions, which is valid for complexes in strong field situations. The structural results and the sharp decrease of $\nu_{NO}$ to *ca.* 1650 $cm^{-1}$ are a consequence of placing the new electron in the antibonding MNO orbital. For iron complexes, the EPR measurements ($S$ = 1/2) and DFT calculations indicate that $Fe^{II}NO^{\bullet}$ is the dominant contribution, revealing that *ca.* 60% of the unpaired electron density is located at the nitrosyl ligand (with two-thirds at nitrogen), with a sizeable metal population of *ca.* 30%. Advanced DFT methodologies have been applied to $[Fe(CN)_5NO]^{3-}$ and its Ru- and Os-analogs for the calculation of the $g$ and hyperfine tensors, taking due account of spin-orbit coupling effects.[36a] The earlier measurements[36b] on

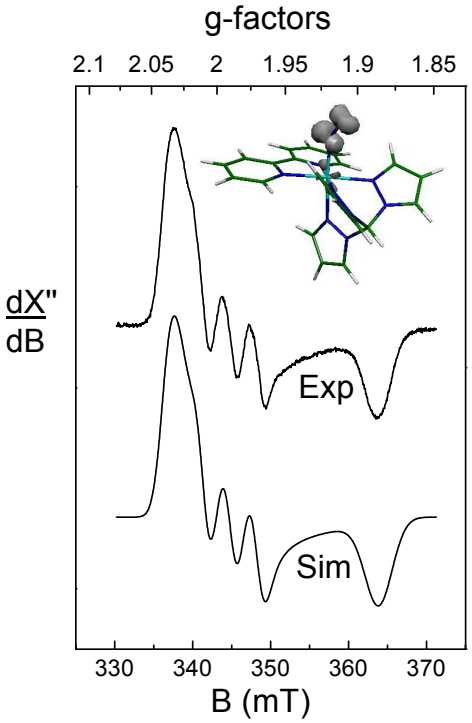


**Figure 2.** EPR spectrum of $[Ru(bpy)(tpm)NO^{\bullet}]^{2+}$. Top right: DFT-calculated spin density in vacuum (B3LYP level, LanLDz basis set). Middle: Spectrum of the electrogenerated cation in MeCN/0.1 M $Bu_4NPF_6$ at 110 ºK. Bottom: Computer simulated spectrum.[38]

$[Fe(CN)_5NO]^{3-}$ have been so confirmed, with a clear differentiation from the related, also paramagnetic $[Fe(CN)_4NO]^{2-}$ compound (see below). Thus, for $[Fe(CN)_5NO]^{3-}$, the values are: exptl (calcd): $g_1$ = 1.99 (2.015); $g_2$ = 1.99 (1.995); $g_3$ = 1.92 (1.893); $A_2$ = 2.8 (3.16). In addition, measurements have been performed with a variety of ruthenium nitrosyl complexes containing different $Ru^{II}X_5$ fragments ($n$ = 7, $S$ = ½, X = amines, py, polypyridines, nitriles, CO, halides, hydride, hydroxide, thiocyanate, cyanide, etc).[37] They all revealed very similar EPR patterns ($g_1$ = 2.015 ± 0.02; $g_2$ = 1.990 ± 0.015; $g_3$ = 1.892 ± 0.03; $g_{av}$ = 1.968 ± 0.02; $\Delta g = g_1 - g_3$ = 0.122 ± 0.037, $A_2$ ($^{14}$N) = 3.3 ± 0.5 mT. Figure 2 shows a representative EPR spectrum of $[Ru(bpy)(tpm)NO]^{2+}$ (tpm = tris(1-pyrazolyl)methane),[38] which is similar to the one for $[Fe(CN)_5NO]^{3-}$.[36b] The rather small variability for the ruthenium complexes differs from the wider range of EPR data reported for iron-nitrosyls with $S$ = ½, pointing to a higher degree of covalency in the $\{RuNO\}^7$ situation than in the corresponding $\{FeNO\}^7$ arrangements, the latter having more accessible options for limiting structures other than $Fe^{II}NO^{\bullet}$, e.g. $Fe^{I}NO^{+}$.

Table 1 includes a representative nitrosyliron complex with $S$ = 3/2, $[Fe(Me_3TACN)(NO)(N_3)_2]$.[23c,d] X-ray absorption, resonance Raman, magnetic circular dichroism and SQUID magnetic susceptibility, together with SCF-Xa-SW calculations support an $Fe^{III}NO^{-}$ distribution, originated in high-spin $Fe^{III}$ ($S$ = 5/2) coupled antiferromagnetically with $NO^{-}$ ($S$ = 1).[23d] This description also holds for complexes containing weak X-coligands, *viz*., aza-macrocycles, [Fe(edta)NO], and some mononuclear non-heme iron proteins.[23d,e] The $\nu_{NO}$ values are somewhat greater than for the $S$ = 1/2 compounds. Interestingly, spin equilibrium $S$ = 1/2 $\rightleftarrows$ $S$ = 3/2, was found for $[Fe(L^{Pr})NO]$ in the solid state. Studies comprising X-ray, EPR, zero- and applied field Mössbauer spectroscopies and DFT calculations support the presence of valence tautomers (redox isomers) rather than a simple high spin $\rightleftarrows$ low spin crossover.[23e]

**c) $n$ = 8**

Well characterized complexes of the $\{MNO\}^8$ class are scarce.[15b,39] Table 1 contains a selected group of compounds. The HNO ligand is predominantly found for $M^{II}$ centers. $NO^{-}$-ligands have been described for some $M^{III}$ complexes with Co(III) and Rh(III),[15b,24b] including a very recent report on nitroxylcob(III)alamin, NOCbl.[40] The reasons for finding $NO^{-}$ or HNO in different coordinative situations are not well understood. The $n$ = 8 systems are very electron-rich, and a facile protonation of bound $NO^{-}$ may be anticipated in aqueous solutions.

The main structural feature is the greater bending of the MNO angle, close to 120º,[15,17] consistent with an increased population of the antibonding orbital (Fig. 1b), as evidenced by the significant decrease of $\nu_{NO}$ to *ca.* 1300 - 1400 $cm^{-1}$ for the $M^{II}$-HNO moieties. The complexes are diamagnetic, with low-spin $d^6$ metal centers and singlet $NO^{-}$ (or HNO).

Remarkably, only one stable iron-nitroxyl complex has been described in aqueous solution, the HNO adduct of myoglobin, $Mb^{II}HNO$.[41] It has been characterized by electrochemistry, NMR, Resonance Raman, XANES and XAFS spectroscopies. Quite relevant to the present Perspective, Table 1 contains data for the theoretically predicted, $[Fe(CN)_5HNO]^{3-}$ complex.[24a] This was calculated as stable, in contrast to the unstable one with bound $NO^{-}$. The relevant structural parameters and IR frequency are consistent with available data for HNO-complexes.[39] A two-electron reduced derivative of SNP had been previously generated electrochemically. It was described as $[Fe(CN)_4(NC)NO]^{3-}$, but the evidence is poor.[41a] Work is currently ongoing to better characterize this important, seemingly nitroxyl-containing complex.[42b]

## Formation and dissociation reactions of $[M^{II,III}(CN)_5NO]^{3,2-}$ and related complexes. Simple ligand interchange or redox-active processes?

Studies on the forward and reverse reactions in eqn. (1) are a point of departure for understanding the coordination chemistry of NO. Analog reactions comprising free aqueous $NO^{+}$ and $NO^{-}$ can not be usually studied, because of faster competitive processes leading to $NO_2^{-}$ and $N_2O$, respectively (see however reference 17).

$$[MX_5H_2O]^x + NO \rightleftarrows [MX_5NO]^x + H_2O \quad k_{on}, k_{off} \quad (1)$$

**Table 2.** Rate constants and activation parameters for the direct ($k_{on}$) and reverse ($k_{off}$) reactions in $[MX_5H_2O]^x + NO \rightleftharpoons [MX_5NO]^x + H_2O$, $T$ = 25 ºC

| Complex precursor | $k_{on}$ $M^{-1}$ $s^{-1}$ $k_{off}$ $s^{-1}$ | $\Delta H^{\neq}$ kJ $mol^{-1}$ | $\Delta S^{\neq}$ J $K^{-1}$ $mol^{-1}$ | $\Delta V^{\neq}$ $cm^3$ $mol^{-1}$ | Ref. |
|---|---|---|---|---|---|
| $[Fe^{II}(CN)_5H_2O]^{3-}$ | $2.5 \times 10^2$ | 70 | 34 | 17.4 | 43 |
| | $1.6 \times 10^{-5}$ | 106.4 | 20 | 7.1 | 43 |
| $[Fe^{II}(H_2O)_6]^{2+}$ | $1.4 \times 10^6$ | 37 | –3 | 6.1 | 44 |
| | $3.2 \times 10^3$ | 48 | –15 | 1.3 | 44 |
| $[Fe^{II}(edta)H_2O]$ | $2.4 \times 10^8$ | 24 | –4 | 4.1 | 45 |
| | 91 | 61 | –5 | 7.6 | 45 |
| $[Fe^{II}(TMPS)]$ | $1.0 \times 10^9$ | 26 | 16 | 2 | 46 |
| | $6.4 \times 10^{-4}$ | | | | 46 |
| $[Fe^{III}(TMPS)(H_2O)_2]$ | $2.8 \times 10^6$ | 57 | 69 | 13 | 46,47 |
| | $0.9 \times 10^3$ | 84 | 94 | 17 | 46,47 |
| $[Fe^{III}(TMPS)(OH)]$ | $1.3 \times 10^4$ | 28 | –71 | –16 | 47 |
| | 7.0 | 90 | 76 | 7.4 | 47 |
| $[Fe^{III}(CN)_5H_2O]^{2-}$ [a] | 0.25 | 52 | –82 | –13.9 | 48 |
| $[Ru^{III}(NH_3)_5H_2O]^{3+}$ [a] | 55.6 | 31 | –108 | | 49 |

[a] Corresponds to the "on" reaction. Undetected dissociation of the NO-complexes.

**Table 3.** Rate constants and activation parameters for the complex-formation ($k_f$) and dissociation ($k_d$) reactions with selected complexes of the $[Fe^{II}(CN)_5L]^{n-}$ series.[a]

| Ligand L | $k_f$ $M^{-1}$ $s^{-1}$ $k_d$ $s^{-1}$ | $\Delta H^{\neq}$ kJ $mol^{-1}$ | $\Delta S^{\neq}$ J $K^{-1}$ $mol^{-1}$ | $\Delta V^{\neq}$ $cm^3$ $mol^{-1}$ | Ref. |
|---|---|---|---|---|---|
| $NO^+$ [b] | | | | | 17-20 |
| CO | 310 [c] | 63 | 15 | | 51a |
| | $< 10^{-8}$ [c,d] | | | | 51a |
| $CN^-$ | 30 [e] | 76.9 | 42 | 13.5 | 51b |
| | $4 \times 10^{-7}$ [c,f] | - | - | - | 51c |
| NO | 250 [c,g] | 70 | 34 | 17.4 | 43 |
| | $1.6 \times 10^{-5}$ [c] | 106 | 20 | 7.1 | 43 |
| dmso | 240 [e] | 64.4 | 16.7 | - | 51d |
| | $7.5 \times 10^{-5}$ [c] | 110 | 46 | - | 51d |
| pz | 380 [h] | 64.4 | 20.9 | - | 51e |
| | $4.2 \times 10^{-4}$ [c] | 110.5 | 58.6 | 13.0 | 51e |
| his | 315 [c] | 64.4 | 21 | 17.0 | 51e |
| | $5.3 \times 10^{-4}$ [c] | 105.4 | 46.0 | - | 51e |
| $NH_3$ | 365/452 [c] | 62/78 | 10/67 | 14.4 | 51f,g |
| | $1.75 \times 10^{-2}$ [c] | 102 | 68 | 16.4 | 51f,g |

[a] $T$ = 25.0 C, unless otherwise stated. [b] Unmeasurable formation reaction and undetectable dissociation reaction. [c] $I$ = 0.1 M. [d] estimated number. [e] $I$ = 1 M. [f] Extrapolated from data reported at higher temperatures. [f] $T$ = 25.4 C. [g] $I$ = 0.5 M.

Table 2 contains the relevant kinetic and mechanistic information from the studies with selected $MX_5$ fragments.[43-49] The pentacyanonitrosylferrates(II)[43] and (III)[48] have provided a unique opportunity for assessing the coordination ability of *low-spin* iron-containing fragments toward NO, in addition to the available studies with Ru-complexes.[50]

With $[Fe^{II}(CN)_5H_2O]^{3-}$, the reaction under excess NO conditions (pH 7) leads to the well characterized $[Fe(CN)_5NO]^{3-}$, eqn. (2), showing a first order rate law in each of the reactants.[43]

$$[Fe^{II}(CN_5H_2O]^{3-} + NO \rightleftharpoons [Fe(CN)_5NO]^{3-} + H_2O \quad k_{on}, k_{off} \qquad (2)$$

The value of $k_{on}$ ($k_{NO}$) = 250 $M^{-1}$ $cm^{-1}$ agrees with the values found for the coordination of several L ligands into the same fragment, *ca.* 200-300 $M^{-1}$ $s^{-1}$ (Table 3).[51] This is indicative of a rate-determining step associated with the release of water from the $Fe^{II}$-center. Considering the similar activation enthalpies, positive activation entropies and the value of the activation volume in reaction (2), which is consistent with the theoretical one for the dissociation of a water molecule, + 13.1 $cm^3$ $mol^{-1}$, a limiting dissociative mechanism (D) has been favored. It appears that the unpaired electron in free NO has no significant mechanistic influence on the coordination toward non redox active metals. This has been rationalized on the basis that, since the odd electron of NO resides in the $\pi^*$ orbital, it does not become involved until the metal-ligand

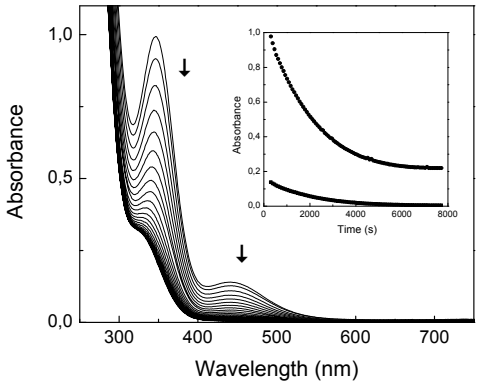


**Figure 3.** Dissociation of NO from $[Fe(CN)_5NO]^{3-}$. UV-vis spectral changes with 0.3 mM reduced SNP, pH 10.2, $[CN^-] = 0.03$ M, $I = 0.1$ M (cycle time 312 s). Inset: Kinetic traces at 347 and 440 nm fitted to a single exponential by SPECFIT, $k_{obs} = 5.14 \times 10^{-4}$ s$^{-1}$, at 50.4 ºC.[43]

bond is largely formed.[16]

Figure 3 shows the successive spectra for the decay of $[Fe(CN)_5NO]^{3-}$ through the dissociation reaction in (2). A value for $k_{off}$ ($k_{-NO}$) = $1.58 \times 10^{-5}$ s$^{-1}$ has been obtained at 25.0 ºC, pH 10.2. The use of excess cyanide conditions was two-fold: as a scavenger for $[Fe(CN)_5H_2O]^{3-}$ and also for $[Fe(CN)_4NO]^{2-}$, by displacing the equilibrium in reaction (3), see below.[43] From activation parameters (Table 2), a D mechanism has also been proposed. By comparing with $k_{-L}$ values in the series of pentacyano(L)-complexes (Table 3), we observe that NO is released faster than $NO^+$, CO or $CN^-$, although slower than other L´s affording weaker σ-π interactions. In fact, the ordering of L in Table 3 reflects the relative positions in the so-called "spectrochemical series", with NO behaving as a moderate-to-strong ligand, although certainly much weaker than $NO^+$, for which no dissociation rate process has ever been detected.

The pH is crucial for assuring that $[Fe(CN)_5NO]^{3-}$ is the predominant nitrosyl species in the aqueous solutions. The $[Fe(CN)_4NO]^{2-}$ ion forms spontaneously in a fast equilibrium,[52] according to eqn. (3):

$$[Fe(CN)_5NO]^{3-} \rightleftharpoons [Fe(CN)_4NO]^{2-} + CN^- \quad (3)$$

Reaction (3) is an example of the *trans*-labilization effect arising in nitrosyl-complexes of the $\{MNO\}^7$ series, which seems crucial for the activation of soluble guanylate cyclase (sGC), an heme-protein that releases *trans*-histidine ensuing very fast NO-coordination, thus starting a chain of events leading to vasodilation.[4,6] To our knowledge, the *trans*-effect has been measured quantitatively only for reaction (3), with $k_3 = 2.7 \times 10^2$ s$^{-1}$, $k_{-3} = 4 \times 10^6$ M$^{-1}$ s$^{-1}$, $K_3 = 6.8 \times 10^{-5}$ M.[52] The low value of $K_3$ indicates that the labilization effect is only modest. The predominance of either the penta- or the tetracyano-nitrosyl complexes in solution can be controlled by changing the pH or the concentration of free cyanide (p$K_a$ = 9.21 for HCN).[43,52]

Table 2 includes some high spin Fe(II) complexes, for which the coordination of NO induces spin pairing. The values of $k_{on}$ and $k_{off}$ were obtained under reversible conditions, by using relaxation- and stopped-flow techniques.[11,16] The values of $k_{on}$ are expectedly much faster than found for reaction (2), showing lower activation enthalpies. The activation entropies and volumes allowed to suggest an $I_d$ mechanism for the complexes with X = $H_2O$,[44] edta[45] and other analogs. An $I_d$ mechanism was also proposed for the "off" reactions. The very fast formation reactions with the heme-complexes were interpreted in terms of a nearly diffusion limited encounter complex formation, $\{Fe^{II}(por)//NO\}$, followed by fast NO-coordination.[46]

In the irreversible reaction of NO with $[Fe^{III}(CN)_5H_2O]^{2-}$,[48] the quantitative product is SNP, described as $Fe^{II}NO^+$, eqn. (4):

$$[Fe^{III}(CN_5)H_2O]^{2-} + NO \rightarrow [Fe(CN)_5NO]^{2-} + H_2O \quad k_{on} \quad (4)$$

The rate law was first order in the reactants, with $k_{on} = 0.25$ M$^{-1}$ s$^{-1}$, many orders of magnitude higher than the values obtained for the coordination of other ligands ($NCS^-$, $N_3^-$, etc) into $[Fe^{III}(CN)_5H_2O]^{2-}$, which are in the range $10^{-4} - 10^{-7}$ M$^{-1}$ s$^{-1}$.[53] The latter reactions have been discussed in terms of an $I_d$ mechanism, and may be catalyzed by Fe(II) or other reductants, associated with the greater lability of water from the Fe(II) centers compared to the Fe(III) ones. In fact, the *lower* activation enthalpy for reaction (4) compared to (2), and the negative values of the activation entropy and volume, exclude the possibility of such an $I_d$ mechanism for reaction (4). The latter may be considered a *reductive nitrosylation* reaction, and it was initially described as an outer-sphere electron transfer process,[48] followed by ligand interchange. This could be objected on the basis of the endergonic character of the one-electron processes involved, and therefore some association of the reactants may be considered. Scheme 1 (left part, steps 1-3) describes the proposed mechanism. The electron transfer step appears as coupled with the substitution of water at the Fe(II) center by $NO^+$ or by the rapidly generated $HNO_2/NO_2^-$ placed in the second coordination sphere.

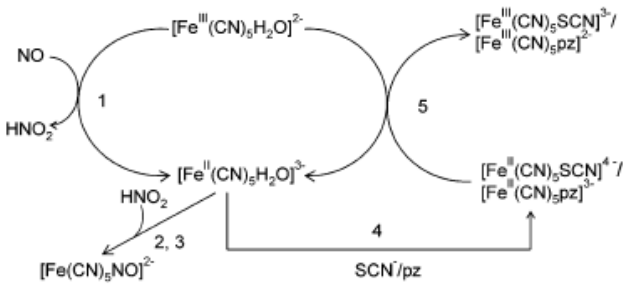


**Scheme 1**

A main point in the proposed mechanism is the intermediacy of $[Fe^{II}(CN_5H_2O]^{3-}$. No direct evidence is available, but competitive experiments with added pyrazine (pz) strongly support a role for $[Fe^{II}(CN_5H_2O]^{3-}$, on the basis of the well disclosed transient formation of $[Fe^{II}(CN)_5pz]^{3-}$ and $[Fe^{III}(CN)_5pz]^{2-}$. As shown in the right part of Scheme 1, the formation of the first complex (step 4) provides strong

**Table 4.** Rate constants and activation parameters for the addition of different nucleophiles (B) into the $[Fe(CN)_5NO]^{2-}$ ion [a]

| Nucleophile B | $k_B$ $M^{-1}$ $s^{-1}$ | $\Delta H^{\#}$ kJ $mol^{-1}$ | $\Delta S^{\#}$ J $K^{-1}$ $mol^{-1}$ | Ref. |
|---|---|---|---|---|
| $OH^-$ | 0.55 | 52.7 | –75 | 56 |
| $NH_3$ | $10^{-4}$ [b] | | | 62a,b |
| $NH_2Et$ | $5.1 \times 10^{-3}$ [c] | 14.6 | –239 | 63 |
| $NH_2OH$ | 0.45 [d] | 37.1 [e] | –13 [e] | 64 |
| $HN_3$ | 0.2 [f] | | | 64 |
| $N_2H_4$ | 0.40 [g] | 26.8 [g] | –163 [g] | 65 |
| $N_2H_3Me$ | $4.4 \times 10^{-2}$ [h] | | | 65 |
| 1,1-$N_2H_2Me_2$ | $6.2 \times 10^{-3}$ [h] | | | 65 |
| $SR^-$ (cys) | $2.6 \times 10^4$ [i] | 31.4 | –54 | 72 |
| $SH^-$ | 170 | 30.1 | –100 | 78a |
| $SO_3^{2-}$ | 450 | 24.3 | –113 | 78b |

[a] $T$ = 25 ºC, $I$ = 1 M, unless otherwise stated. [b] pH 10-13. [c] pH 8.6-9.6. [d] Value calculated at pH 8 from the third order rate law. [e] Calculated from the reported data. [f] $T$ = 23 ºC, pH 6. [g] pH 9.2. [h] pH 6-10. [i] $I$ = 0.4 M.

evidence for the aqua-precursor (pz competes with $HNO_2/NO_2^-$), whilst the second-complex is formed through a fast reaction of $[Fe^{II}(CN)_5pz]^{3-}$ with the initial reactant, $[Fe^{III}(CN)_5H_2O]^{2-}$ (step 5). Similar results have been obtained with $NCS^-$ as the competing scavenger for $[Fe^{II}(CN_5H_2O]^{3-}$. Note that the reactions between $[Fe^{III}(CN_5)H_2O]^{2-}$ and $pz/NCS^-$ under similar conditions but in the absence of NO are orders of magnitude slower.

In a complementary attempt aiming to cover the substitution behavior of $[Fe^{III}(CN)_5L]^{n-}$ analogs (L = py, $CN^-$, $NO_2^-$), the reactions with NO led to distinctive reaction rates.[48] With L = py, the initial, slowly increasing formation of $[Fe^{II}(CN)_5py]^{3-}$, coupled to the formation and further decay of $[Fe^{III}(CN)_5py]^{2-}$, indicate that a first reduction of Fe(III) by NO is operative. The $[Fe^{II}(CN)_5py]^{3-}$ complex also decays in longer time scales, leading to SNP. For L = $CN^-$, a very slow decay of $[Fe^{III}(CN)_6]^{3-}$ was observed, with SNP appearing in the time scale of hours. This must be related to the great stability and inertness of $[Fe^{II}(CN)_6]^{4-}$. In remarkable contrast, $[Fe^{III}(CN)_5NO_2]^{3-}$ evolved to SNP in a stopped-flow time scale, suggesting that $Fe^{II}$-$NO^+$ forms without Fe-N bond cleavage, *i.e.*, subsequent to the electron-transfer step and proton assisted dehydration of bound nitrite.

The mechanism for reaction (4) has been critically discussed[12,50] in the context of close similarities with the results found for the reactions of NO with low spin $[Ru^{III}(NH_3)_5L]$ complexes (L = $H_2O$, $Cl^-$, $NH_3$, see Table 2). An associative bond formation of NO coupled to a concerted electron transfer step to produce final $[Ru^{II}(NH_3)_5(NO^+)]^{3+}$ has been proposed,[49] as an alternative route to the limiting associative (A) mechanism discussed earlier for the reaction of NO with $[Ru^{III}(NH_3)_6]^{3+}$.[54]

The results and mechanistic interpretation for the Fe(III) cyano-complexes differ with those for the high spin systems containing Fe(III)-porphyrins.[12,15] In contrast with the irreversible character of the forward reaction in (4), a reversible behavior has been found for the heme-complexes. Dissociative (D or $I_d$) mechanisms have been proposed for the formation and the dissociation reactions of the respective NO-complexes with $[Fe^{III}(por)(H_2O)_2]^x$.[16] It has been currently accepted that the formation reactions are rate-controlled by the release of bound water. However, recent work has demonstrated that the detailed mechanisms are dependent on pH, based on the possible deprotonation at one of the $H_2O$ ligands.[47] Table 2 shows that the replacement of $H_2O$ by $OH^-$ reflects in significant differences in the activation parameters and volumes, with the onset of associative mechanisms (A), involving strong electronic rearrangements (spin redistributions) for both the "on" and "off" reactions. A closer look to these emerging studies reveals the influence of the coordination number (5 or 6), type and overall charge of the porphyrin-chelate, nature of the substituents on the ring, solvent conditions, etc.[55]

## Electrophilic reactivity of bound $NO^+$ in SNP and related complexes

For the $\{MNO\}^6$ complexes, a characteristic type of reactivity involves the reversible addition of nucleophiles B to the $NO^+$-ligand, as in reaction (5):

$$[MX_5NO]^x + B \rightleftharpoons [MX_5N(O)B]^x \quad (5)$$

The overall stoichiometries have been studied for a vast amount of metals (mainly ruthenium) and X coligands ($NH_3$, $Cl^-$, polypyridines, etc), by using different nucleophiles like $OH^-$, *S*-binding species ($SR^-$, $SH^-$ or $SO_3^{2-}$), *N*-binding bases ($NH_3$, amines, $NH_2OH$, $HN_3$, $N_2H_4$), and others.[13,18] Some equilibrium constants have been measured, though few kinetic and mechanistic studies have been performed, with the remarkable exception of SNP. Table 4 shows the results for the reactions of different nucleophiles with SNP.

### i) Reactions with $OH^-$ as a nucleophile

A relatively simple process occurs in the reaction with $OH^-$, with no redox events, comprising two reversible reactions (6,7):[56]

$$[Fe(CN)_5NO]^{2-} + OH^- \rightleftharpoons [Fe(CN)_5NO_2H]^{3-} \quad k_6, k_{-6} \quad (6)$$

$$[Fe(CN)_5NO_2H]^{3-} + OH^- \rightleftharpoons [Fe(CN)_5NO_2]^{4-} + H_2O \quad (7)$$

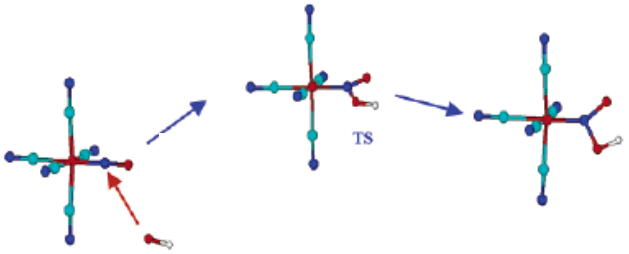


**Figure 4.** DFT-optimized geometries for the initial steps of the reaction of $[Fe(CN)_5NO]^{2-}$ with $OH^-$, giving the transition state and the nitrous acid intermediate $[Fe(CN)_5NO_2H]^{3-}$.[58]

The kinetic and mechanistic studies afforded a first order rate law in complex and $OH^-$, with $k_{2nd}$ = 0.55 $M^{-1}$ $s^{-1}$ (25 ºC, $I$ = 0.1 M), $\Delta H^{\neq}$ = 53 kJ $mol^{-1}$ and $\Delta S^{\neq}$ = –49 J $K^{-1}$ $mol^{-1}$. This was interpreted as a rate-limiting forward process in (6), followed by a rapid deprotonation of the nitrous acid intermediate in (7). Thus, $k_{2nd}$ might be equalized to $k_6$.

In subsequent work with the ruthenium-[57] and osmium-analogs,[22g] as well as with the highly reactive $[Ru(bpy)(tpm)NO]^{3+}$,[38] studies in a broad pH-range displayed a more complex rate law, namely: $k_{obs} = k_{OH}\{[OH^-] + 1/K_{eq}[OH^-]\}$, which simplifies to $k_{obs} = k_{OH} \times [OH^-]$ at sufficiently high pHs.[22g] From a mechanistic analysis including an ion-pair formation event ($K_{ip}$) coupled to reaction (6), $k_{OH}$ values could be adequately fitted, thus providing for the calculation of $k_{ad}$ ($s^{-1}$), the elementary addition step for the conversion of the ion-pair into the adduct intermediate ($k_{OH} = K_{ip} \times k_{ad}$). Although no direct evidence exists for the nitrous acid intermediate, DFT calculations have provided the optimized geometries along the reaction coordinate for the reactant and product in reaction (6), including the transition state (Fig. 4).[58] The process can be described as an addition of an electron pair of $OH^-$ to the LUMO, with a formal conversion from $n$ = 6 to 8 in the $\{FeNO\}^n$ moiety. The geometrical and IR parameters calculated for the different species are in agreement with the proposed scheme.

The influence of changing the $MX_5$ fragment has been investigated through the reactions of a comprehensive set of $[MX_5NO]^x$ complexes with $OH^-$.[58] All of them afford the same global stoichiometry as described in reactions (6-7), with formation of the corresponding nitro-complexes. The rate constants for the nucleophilic addition step $k_6$ may be equalized to $k_{OH}$, covering a wide range of *ca.* 10 orders of magnitude, depending on the oxidizing capability of the $NO^+$-ligand, as measured by the redox potentials, $E_{NO+/NO}$, which also display a wide range, > 1.0 V. Figure 5 shows a correlation of ln $k_{OH}$ against $E_{NO+/NO}$. It represents a linear-free-energy-relationship (LFER), as currently described for the behavior of a set of reactions governed by a common mechanism.[13] Marcus demonstrated that this type of relation holds for the outer-sphere, cross redox reactions of coordination compounds (with a theoretical slope of 19.4 $V^{-1}$), and also extended this approach to inner-sphere reactions as well, which is the present case for the nucleophilic additions.[59] Some complexes of the $[Ru(py)_4(L)NO]^x$ series deviate from the main line, although with a similar slope, probably because of steric restrictions.

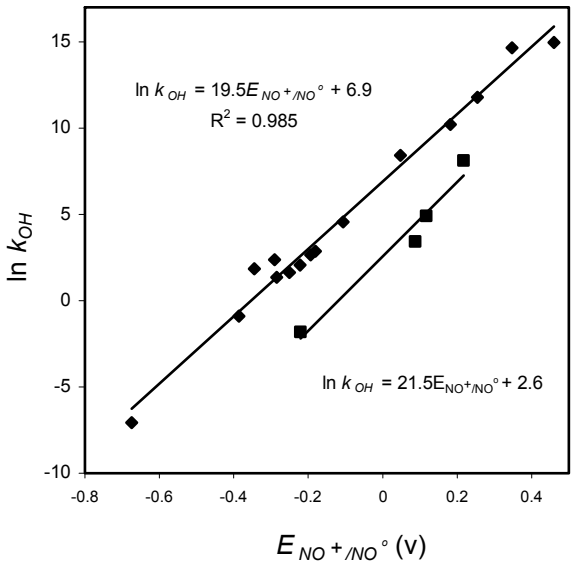


**Figure 5.** Plot of ln $k_{OH}$ (addition rate constant) against $E_{NO+/NO}$ (V *vs* Ag/AgCl,3M $Cl^-$) for the reactions of $[MX_5NO]^x$ complexes with $OH^-$. Main plot, from left to right, in order of increasing potentials: $[Os(CN)_5NO]^{2-}$; *trans*-$[Ru(his)(NH_3)_4NO]^{3+}$; $[Ru(CN)_5NO]^{2-}$; $[Ru(edta)NO]$; $[Fe(CN)_5NO]^{2-}$; *trans*-$[Ru(4\text{-}Mepy)(NH_3)_4NO]^{3+}$; *trans*-$[Ru(NH_3)_4NO(py)]^{3+}$; *trans*-$[Ru(Clpy)(NH_3)_4NO]^{3+}$; *trans*-$[Ru(NH_3)_4NO(nic)]^{3+}$; *trans*-$[Ru(NH_3)_4NO(pz)]^{3+}$; *cis*-$[Ru(bpy)_2ClNO]^{2+}$; $[Ru(bpy)(trpy)NO]^{3+}$; *cis*-$[Ru(bpy)_2ClNO]^{2+}$; *cis*-$[Ru(AcN)(bpy)_2NO]^{3+}$; $[Ru(bpy)(tpm)NO]^{3+}$. Secondary plot: *trans*-$[Ru(OH)NO(py)_4]^{2+}$; *trans*-$[RuClNO(py)_4]^{2+}$; *trans*-$[Ru(NCS)NO(py)_4]^{2+}$; *trans*-$[NCRu(py)_4CNRu(py)_4NO]^{3+}$.[58]

The onset of Fig. 5 illustrates a predictive situation for nitrosyl-coordination compounds, with the electrophilic reactivity being controlled by the one-electron nitrosyl-redox potential, a parameter that carries all the information on the electronic density at the MNO fragments, influenced by the X coligands. It can be seen that SNP, as well as its Ru- and particularly Os-analogs, are among the *least* electrophilic compounds, which is equivalent to say that they show a lower degree of "nitrosonium character" along the series. In fact, cyanides behave as poorly $\pi$*-acceptor ligands, competing with $NO^+$, and are considered to be strong $\sigma$-donors, [26b] favoring electron-rich MNO moieties. On the other hand, the positively charged complexes with electron-acceptor coligands and high $E_{NO+/NO}$ values behave as strongly electrophilic.[38] Despite the uncertainties with the appropriate $E_{NO+/NO}$ values for the nitrosyl ferri-hemes, measurements of $OH^-$ additions to $Hb^{III}NO$ and $Mb^{III}NO$,[11] and recently estimated $k_{OH}$ values with an iron-porphyrin[60] support the validity of the correlation for this group of compounds.

**ii) Reactions with N-binding nucleophiles**

Small nitrogenated molecules are also active nucleophiles toward bound $NO^+$.[18,61] Table 4 includes data for reactions (8-12), representing the overall stoichiometries for B = ammonia,[62] aliphatic amines,[63] hydroxylamine,[64] hydrazoic acid[64] and hydrazine[65] reacting with SNP in aqueous solutions:

$$[Fe(CN)_5NO]^{2-} + NH_3 + OH^- \longrightarrow [Fe(CN)_5H_2O]^{3-} + N_2 + H_2O \quad (8)$$

$$[Fe(CN)_5NO]^{2-} + NH_2R + OH^- \longrightarrow [Fe(CN)_5H_2O]^{3-} + N_2 + ROH \quad (9)$$

$$[Fe(CN)_5NO]^{2-} + NH_2OH + OH^- \longrightarrow [Fe(CN)_5H_2O]^{3-} + N_2O + H_2O \quad (10)$$

$$[Fe(CN)_5NO]^{2-} + HN_3 + OH^- \longrightarrow [Fe(CN)_5H_2O]^{3-} + N_2 + N_2O \quad (11)$$

$$[Fe(CN)_5NO]^{2-} + N_2H_4 + OH^- \longrightarrow [Fe(CN)_5H_2O]^{3-} + N_2O + NH_3 \quad (12)$$

The mechanisms of reactions (8-12) may also be described as additions of the *N*-atom of the nucleophile on the $NO^+$ ligand, coupled with deprotonation, as suggested by pH-dependent rate laws with a first order behavior in complex- and nucleophile-concentrations. The negative activation entropies sustain an associative mechanism. Further adduct-reorganizations generate the different gaseous products, $N_2$ and/or $N_2O$. Theoretical (DFT) characterization of the adduct intermediates has been reported.[61]

Reaction (8) was studied at pHs ≥ 10, in order to avoid the competition of reactions (6,7). Table 4 shows that the rate constants have comparatively low values, as is also the case for reaction (9). A mechanism comprising a rapid adduct-formation equilibrium, followed by slow reorganization leading to the gaseous products can be assumed.[62,63] The latter event probably requires deprotonation of the bound amine in the adduct. The additions of primary amines on SNP have also been studied in nonaqueous (organic) media, in order to favor the stabilization and controlled reactivity of coordinated diazonium ions, as well as for elucidating the possible role of SNP as a nitrosating agent in lipophilic media.[66]

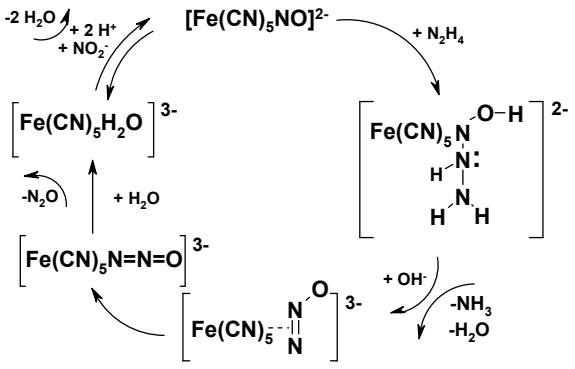


**Scheme 2**

A comprehensive kinetic and mechanistic work has been reported for reaction (12).[65] Scheme 2 describes the proposed steps for the addition of $N_2H_4$ ($k_{N2H4}$ = 0.43 $M^{-1}$ $s^{-1}$, pH 9.4, 25 ºC), with subsequent deprotonation and N-N cleavage, leading to $NH_3$ and to the side-on $\eta^2$-$N_2O$ and end-on $\eta^1$-$N_2O$ isomers. The products are free $N_2O$ and $[Fe(CN)_5H_2O]^{3-}$, which is able to further coordinate more nitrite (as $NO^+$).

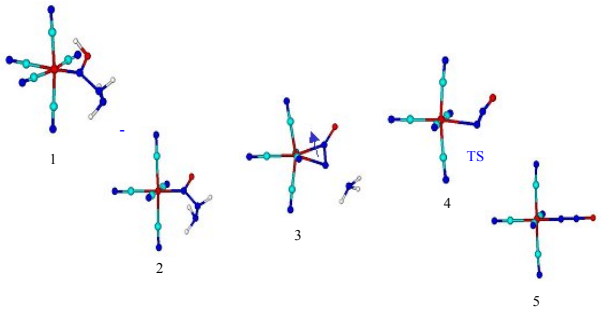


**Figure 6.** DFT-calculated geometries in the initial steps of the reaction of $[Fe(CN)_5NO]^{2-}$ with hydrazine, rendering the $N_2O$-bound intermediates. The structures correspond to singular points in the potential hypersurface, calculated at a B3LYP/6-31G** level. Relative energies (y-coordinate) are not drawn to scale. From left to right: 1: $[(NC)_5FeN(OH)NHNH_2]^{2-}$; 2: $[(NC)_5FeN(O)NHNH_2]^{3-}$; 3: $[(NC)_5Fe\text{-}\eta^2\text{-}N_2O]^{3-}$; 4: TS structure. 5: $[(NC)_5Fe\text{-}\eta^1\text{-}N_2O]^{3-}$.[65]

Thus, a catalytic reduction of nitrite by hydrazine ensues in the appropriate conditions. Interestingly, alternative $N_2H_4$-additions to other nitrosyl complexes leading to azide-complexes (not $N_2O$) have been reported.[18] The attack of *N*-binding nucleophiles on bound $NO^+$ is at the heart of the mechanisms of nitrite reductions in soils by bacteria and reducing enzymes, evolving to gaseous products, $N_2/N_2O$. In the nitrite reductases, nitrite-coordination at Fe(II) heme-centers (forming $NO^+$) is considered the first step toward further reactivity.[67]

Reaction (12) has been studied using labeled SNP ($^{15}NO$), with the result that the gaseous product has been quantitatively identified as $^{14}N^{15}NO$, with no label at $NH_3$. This fact, together with DFT evidence shown in Fig. 6 supports the proposed Scheme 2. The prediction of the $N_2O$-linkage isomers is a novel result. Direct spectroscopic evidence exists only for the coordination of $\eta^1$-$N_2O$ on some Ru- and Os-complexes.[8] The intermediacy of $\eta^2$-$N_2O$ and $\eta^1$-$N_2O$ in reaction (12) is supported by the geometrical and IR parameters derived from the DFT treatment.

In the reactions of Me-substituted derivatives of hydrazine adding to SNP, closely related stoichiometries leading to $N_2O$ have been found for methylhydrazine and 1,1-dimethylhydrazine, also forming methylamine and dimethylamine, respectively (cf. reaction (12)).[65] The related mechanisms support an attack *through the $NH_2$ groups*, with the rates decreasing by about a factor of 10 for each Me-substitution (Table 2). A parallel path with a different product distribution has been found for methylhydrazine at pHs > 8, eqn. (13). The proposed mechanism involves an adduct formation through the *N*-atom *vicinal to the Me group*, which reacts with another $[Fe(CN)_5NO]^{2-}$ giving a dimer that may further rearrange by cleavage at the N-N bond and displacement of the Me group.

$$2[Fe(CN)_5NO]^{2-} + H_2NNHMe + 2OH^- \rightarrow 2[Fe(CN)_5H_2O]^{3-} + N_2 + N_2O + MeOH \quad (13)$$

Quite interestingly, the reaction of SNP with 1,2-dimethylhydrazine follows a different route, with a drastically different stoichiometry, eqn. (14). It comprises a *full six-electron reduction* of nitrosyl to $NH_3$, and the formation of azomethane.[65]

$$[Fe(CN)_5NO]^{2-} + 3MeHNNHMe \rightarrow [Fe(CN)_5NH_3]^{3-} + H_3O^+ + 3MeNNMe \quad (14)$$

The mechanism in reaction (14) probably involves two-electron reduced intermediates, $[Fe(CN)_5HNO]^{3-}$ and $[Fe(CN)_5NH_2OH]^{3-}$, in contrast with the conversion of $NO^+$ to $N_2O$ in (12), when using $N_2H_4$ or other Me-derivatives.

In the context of the reductive nitrosylation studies with the ferri-hemes, recent pioneering results allowed to include $NO_2^-$ as a potential nucleophile adding to the electrophilic $\{FeNO\}^6$ moieties.[68] $NO_2^-$ is a ubiquitous impurity in NO-solutions because it is the product of NO autoxidation.[69] Its role in biochemistry is being revisited, by considering it as a possible vascular storage pool of NO mediated by the reduction of $NO_2^-$ with Hb.[12,16] When solutions of diverse $[Fe^{III}(por)(H_2O)_2]^x$ complexes, (por = TPPS, TMPyP, as well as metHb and metMb) were made to react with NO in the presence of varying amounts of added $NO_2^-$ at moderately acidic pHs (4–5), greater rates of reductive nitrosylation were obtained.[16c] From the dependence of $k_{obs}$ on the concentration of $NO_2^-$, values of $k_{nitrite}$ have been calculated. They are in the range $1.1 \times 10^{-2}$ to $2.4 \times 10^2$ $M^{-1}$ $s^{-1}$.[70] They show a similar trend as found for the $OH^-$-additions, in the sense that the rate constants increase with the positive charge on the porphyrins.[12] However, by comparing the rate-constant values, the nucleophilic ability of $NO_2^-$ turns out to be significantly lower than for $OH^-$ , by several orders of magnitude. Both $NO_2^-$ and $HNO_2$ contribute to the rates, with $NO_2^-$ being faster by a factor of two. In the mechanistic analysis, $N_2O_3$ has been proposed as the initial bound adduct-intermediate, as described in a general way by eqn. (5). $N_2O_3$ should be released very fast and hydrolyzed to $NO_2^-$ or $HNO_2$, depending on pH. The possible, similar nitrite-addition to SNP has not been studied, it being expected to be very slow, by comparing with the above data for the iron nitrosyl-porphyrins.

The addition of Angeli's salt (sodium trioxodinitrate, $N_2O_3^{2-}$) to SNP has been studied spectrophotometrically in the pH range 5-11, with analysis of the gaseous products NO and $N_2O$, and using labeled trioxodinitrate ($^{15}N$).[71] The reaction starts by the addition of $N_2O_3^{2-}$ to SNP, involving the cleavage of the N=N bond of the reactant, with formation of free nitrite and a dinitrosyl adduct, reaction (15). The adduct converts to an intermediate absorbing at 410 nm, with release of NO, and, in a slower time scale, $N_2O$.

$$[Fe(CN)_5NO]^{2-} + N_2O_3^{2-} \rightarrow [Fe(CN)_5N_2O_2]^{3-} + NO_2^- \quad (15)$$

Reaction (15) involves the formal addition of $NO^-$ to SNP. The mechanism has been critically reviewed,[13] and merits to be revisited, looking for a more reliable characterization of intermediates under anaerobic conditions, with a due consideration of reaction (3) in the studied pH range. Angeli's salt is a recognized nitroxyl-donor,[39b] and the reaction is quite representative of very significant redox interconversions among the different redox states of bound nitrosyl.

**iii) Reactions with S-binding nucleophiles**

The reactions of SNP with cysteine and related thiols (HSR) have been studied by using stopped-flow and T-jump techniques.[72] Reaction (16) describes the addition process, which requires thiol-deprotonation. The electronic absorption maxima of the red products lie at 522-526 nm, with $\varepsilon_{max}$ values of *ca.* $10^3$-$10^4$ $M^{-1}$ $cm^{-1}$. The absorptions may be traced to metal-to-ligand charge transfer transitions to the *bent* nitrosothiolate ligands, N(O)SR.

$$[Fe(CN)_5NO]^{2-} + RS^{n-} \rightleftharpoons [Fe(CN)_5N(O)SR]^{(n+2)-} \quad k_{16}, k_{-16} \quad (16)$$

The IR evidence aids in the identification of $[Fe(CN)_5N(O)SR]^{3-}$. For R = Et, $\nu_{NO}$ = 1350 $cm^{-1}$,[73] suggesting a double bond character in NO (compare N(O)SR with nitroxyl, HNO). The first crystalline structure in this family of metal-bound nitrosothiolates has been recently published for the stable *trans*-$K[IrCl_4(CH_3CN)N(O)SCH_2Ph]$.[74] The rate-laws for the forward processes in reactions (16) were first order in each reactant, and first order for the reverse adduct-decomposition,[72] with $k_{16}$ ($k_{SR}$) and $k_{-16}$ in the range $10^3 - 10^4$ $M^{-1}$ $s^{-1}$ (Table 4) and $10^1 - 10^3$ $s^{-1}$, respectively. The $k_{SR}$ values are significantly greater than the previously analyzed ones for $OH^-$ and nitrogen hydrides, probably because of the more polarizable character of the sulfur-binding nucleophiles.

The nitrosothiolate adducts appear as only moderately stable toward back-dissociation, depending on the thiolate ($K_{16} \approx 10^2$ $M^{-1}$).[72] The red adducts may also decay through subsequent redox processes,[75] with the rates strongly dependent on the thiolate-substituents and on the relative ratios of SNP/thiolate.[75b,76] The reactions of SNP with cysteine and other thiolates have been studied in detail, at pH 10.[76] Spontaneous intramolecular redox decompositions agree with eqn (17), with $k_{17} \approx 10^{-3}$ $s^{-1}$, in excess of SNP. The decomposition rates increase with excess thiolate, with autocatalytic processes involving $RS^{\bullet(n-1)-}$ and $RSSR^{\bullet(2n-1)-}$ radicals.[76] In any case, the final products of $NO^+$-reduction are the EPR active $[Fe(CN)_5NO]^{3-}$ and the disulfide, a main sink for the thiyl radical.

$$[Fe(CN)_5NOSR]^{(n+2)-} \rightarrow [Fe(CN)_5NO]^{3-} + RS^{\bullet(n-1)-} \quad (17)$$

Recently, a comprehensive kinetic study in the stopped-flow regime has been carried out for the reactions of a set of $[Ru^{II}X_5(NO^+)]^x$ complexes with cysteine (X = polypyridines, $NH_3$, edta, etc).[77] The reactions showed to be complex, and different processes could be identified for increasing time scales. Scheme 3 has been proposed for the successive additions of *two* cysteinate ions, followed by a final intramolecular redox process that leads to the ruthenium aqua ion, $[Ru^{II}X_5H_2O]^x$, $N_2O$ and cystine.

The two-electron reduction of $NO^+$ for the ruthenium-nitrosyl complexes contrasts with the one-electron process observed with SNP, eqn. (17). This has been tentatively attributed to the more oxidizing capability of the ruthenium nitrosyls. Figure 7 displays two LFER plots, similar as those presented in Fig. 5. The upper trace relates to the faster

processes associated with the addition of the first cysteinate; it

$$[X_5RuNO]^n \underset{-RS^-}{\overset{RS^-}{\rightleftharpoons}} [X_5RuN(O)SR]^{n-1} \underset{-RS^-}{\overset{RS^-}{\rightleftharpoons}} [X_5RuN(O)(SR)_2]^{n-2} \rightarrow [X_5Ru(H_2O)]^{n-1} + ½\ N_2O + RSSR$$

**Scheme 3**

can be seen that points 5-9 deviate from the straight line because of approaching the diffusion control limit. The points 1-4, however, are aligned with a slope close to the theoretically predicted value, revealing a similar situation as the one discussed previously for $OH^-$. The lower trace can be associated with the reaction of the second cysteinate, and provides valuable evidence for the ongoing nucleophilic process. Further studies with thiolate-additions may be relevant for disclosing which are the factors controlling the appearance of one- or two-electron reduction products of $[MX_5(NO^+)]^x$.

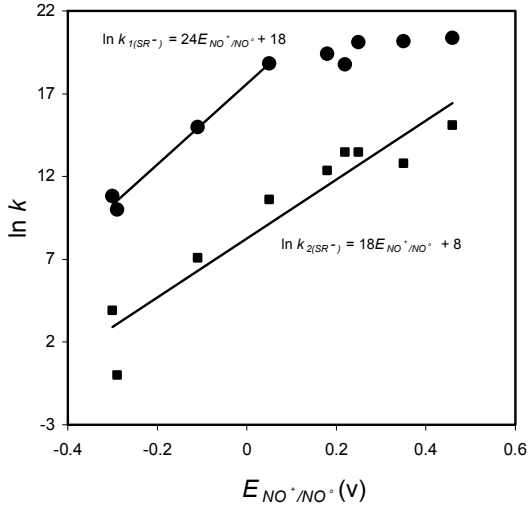


**Figure 7.** Plot of ln $k_{1(SR)}$ and ln $k_{2(SR)}$ against $E_{NO+/NO}$ (V *vs* Ag/AgCl,3M $Cl^-$) for the addition reactions of cysteine on a series of $[RuX_5NO]^x$ complexes. In both plots, from left to right: $[Fe(CN)_5NO]^{2-}$(down); $[Ru(edta)NO]^-$ (up); *trans*-$[Ru(NH_3)_4NO(pz)]^{3+}$; *cis*-$[Ru(bpy)_2ClNO]^{2+}$; *cis*-$[Ru(bpy)_2(NO_2)NO]^{2+}$; *trans*-$[NCRu(py)_4CNRu(py)_4NO]^{3+}$; *cis*-$[Ru(bpy)(trpy)NO]^{3+}$; *cis*-$[Ru(AcN)(bpy)_2NO]^{3+}$; $[Ru(bpz)(trpy)NO]^{3+}$.[77]

The reactions of other *S*-nucleophiles ($SH^-$ and $SO_3^{2-}$) have been studied with SNP (Table 4).[78] Both agree with the general scheme in reaction (5) for the first nucleophilic addition step. The elucidation of the nature of the adduct-intermediates and the decomposition modes would probably merit a revision of these reactions.

## Nucleophilic reactivity of bound NO•. The reactions with $O_2$

One of the possible routes for the decay of free NO in biologically relevant aqueous solutions is through the reaction described by eqn. (18):[16]

$$4NO + O_2 + 2H_2O \rightarrow 4H^+ + 4NO_2^- \quad (18)$$

The rate law in reaction (18) is second-order in NO and first order in $O_2$, with $k_{18} = 2.88 \times 10^6\ M^{-2}\ s^{-1}$.[69] Thus, NO is expected to survive a long time under the dilute NO concentrations in the bodily fluids, unless immune response conditions are generated, or other sinks for faster NO consumption are available.[16] The question is how the reactivity of NO toward $O_2$ is modified by coordination to transition metals, which may be certainly present in the biological fluids. Remarkably, no detailed kinetic and mechanistic studies on the reactions of $\{MNO\}^7$ complexes with $O_2$ have been available,[16,17] with the exception of the autoxidation of $Mb^{II}NO$, leading to metMb and $NO_3^-$ in aerated media.[79]

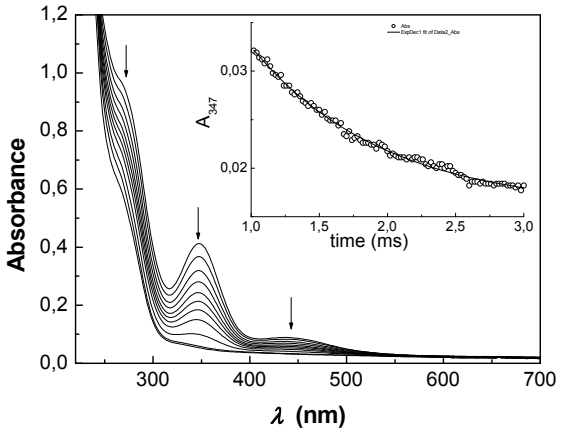


**Figure 8.** Reaction of $O_2$ with the $[Fe(CN)_5NO^\bullet]^{3-}$ ion. (a) Successive UV-vis spectra for the titration of $10^{-4}$ M $[Fe(CN)_5NO^\bullet]^{3-}$ with $2.6 \times 10^{-4}$ M $[O_2]$; pH 10, $I = 0.1$ M; excess cyanide, $5 \times 10^{-4}$ M; $T = 25$ ºC. Inset: Stopped-flow trace for the decay of $[Fe(CN)_5NO^\bullet]^{3-}$, at 347 nm.[80]

In the same way as electrophilic reactivity can be predicted for $NO^+$-complexes, we may anticipate a nucleophilic reactivity for the more electron-rich NO-complexes. Although nitrosyl protonation reactions seem not to occur at the $\{MNO\}^7$ moieties, some complexes have been proved to be oxygen-sensitive.[16] A study on the autoxidation reaction of $[Fe(CN)_5NO]^{3-}$ in aqueous solution has been performed very recently.[80] Figure 8 shows the decay of $[Fe(CN)_5NO]^{3-}$ with successive additions of dissolved $O_2$. The following stoichiometry has been established, eqn. (19)

$$4[Fe(CN)_5NO]^{3-} + O_2 + 2H_2O \rightarrow 4[Fe(CN)_5NO]^{2-} + 4OH^- \quad (19)$$

In excess of dissolved $O_2$, $[Fe(CN)_5NO]^{3-}$ decays exponentially in a stopped-flow timescale (inset Fig. 8). The pseudo-first order rate constant $k_{obs}$ correlates linearly with $[O_2]$, leading to a global second-order rate law: $-1/4d[Fe(CN)_5NO^{3-}]/dt = k_{19}[Fe(CN)_5NO^{3-}][O_2]$, with $k_{19} = (3.5 \pm 0.2) \times 10^5\ M^{-1}\ s^{-1}$ at 25ºC, pH 10. The activation parameters were: $\Delta H^{\#} = 40$ kJ mol$^{-1}$, $\Delta S^{\#} = 12$ J K$^{-1}$ mol$^{-1}$. An excess of free $CN^-$ had to be used to minimize *trans*-labilization of this ligand, eqn. (3). The rate constant was

insensitive to changes in pH (9–11) and ionic strength (0.1–1 M). Noticeably, the oxidation rate *decreased* markedly for pH < 10 in the absence of cyanide.

The above results cannot be accommodated by an outer-sphere mechanism because of the endergonic character of the first one-electron transfer process for the formation of SNP and superoxide, $O_2^-$. Alternative $O_2$-coordination steps following the dissociation of NO or $CN^-$ have also been discarded. Instead, an associative route through reactions (20-21) has been proposed for the initial steps.

$$[Fe^{II}(CN)_5NO]^{3-} + O_2 \underset{k_{-ad}}{\overset{k_{ad}}{\rightleftharpoons}} [Fe^{III}(CN)_5N(O)O_2]^{3-} \quad (20)$$

$$[Fe^{III}(CN)_5N(O)O_2]^{3-} + [Fe(CN)_5NO]^{3-} \rightarrow 2[Fe(CN)_5NO_2]^{3-} \quad (21)$$

In reaction (20) a new covalent bond forms between bound NO and $O_2$. The product has been described as a peroxynitrite anion bound to Fe(III), Fig. 9, according to DFT computations.

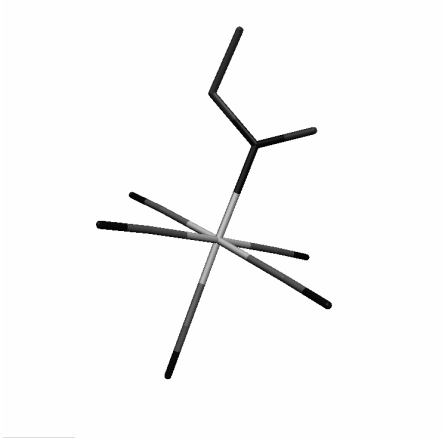

**Figure 9.** DFT-optimized geometry of the Fe(III)-peroxynitrite adduct formed in the initial step of the reaction of $[Fe(CN)_5NO^{\bullet}]^{3-}$ with $O_2$. Spin densities indicate low spin Fe(III), $d^5$, and bound peroxynitrite anion (not low spin Fe(II) + nitrosyldioxyl radical).[80]

For the reaction of $Mb^{II}NO$ with $O_2$, an isomerization of the peroxynitrite adduct has been proposed in order to explain the formation of $NO_3^-$ as a final product.[79] Instead, we propose the fast bimolecular formation of $[Fe(CN)_5NO_2]^{3-}$, eqn. (21), with a subsequent reaction (22):

$$[Fe(CN)_5NO_2]^{3-} + [Fe(CN)_5NO]^{3-} + H_2O \rightarrow 2[Fe(CN)_5NO]^{2-} + 2OH^- \quad (22)$$

Both reactions (21) and (22) probably involve several steps. The oxidation equivalents remain bound to the metal all along the reaction, leading to the experimentally found 4:1 global stoichiometry, without other detectable by-products. By assuming steady state conditions for $[Fe^{III}(CN)_5N(O)O_2]^{3-}$ we get $-d[Fe(CN)_5NO^{3-}]/dt = 4k_{ad}k_{21}[O_2][Fe(CN)_5NO^{3-}]^2/(k_{-ad} + k_{21}[Fe(CN)_5NO^{3-}])$. With $k_{21}[Fe(CN)_5NO^{3-}] > k_{-ad}$, this expression reduces to the observed first order rate law in each reactant, with $k_{19} = k_{ad}$.

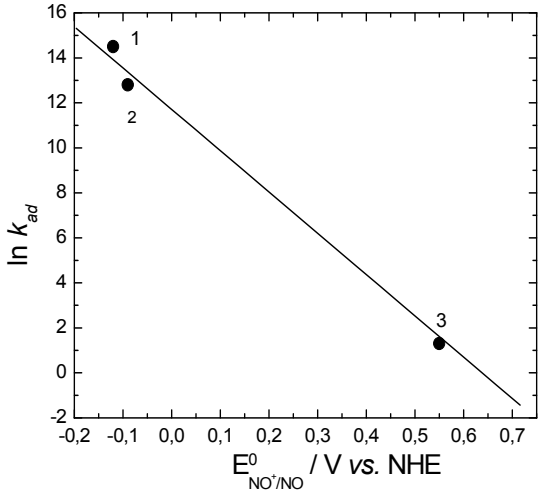


**Figure 10.** Plot of ln $k_{ad}$ vs $E_{NO^+/NO}$ for the reactions of $O_2$ with different complexes: (1) $[Ru^{II}(NH_3)_5NO]^{2+}$, (2) $[Fe^{II}(CN)_5NO]^{3-}$ and (3) $[Ru^{II}(bpy)(tpm)NO]^{2+}$.[80]

Second order rate laws have been also found for the $[Ru(bpy)(tpm)NO]^{2+}$ and $[Ru(NH_3)_5NO]^{2+}$ complexes[38,81] reacting with $O_2$.[17] As the spin density distribution along the different $\{MNO\}^7$ moieties remains essentially invariable,[37] we should expect similar reactivity patterns for the NO-complexes. The $[Fe(CN)_5NO]^{3-}$ and $[Ru(NH_3)_5NO]^{2+}$ complexes (affording $E_{NO+/NO}$ values near to –0.10 V) react with very similar addition rate constants. However, the $[Ru(bpy)(tpm)NO]^{2+}$ ion ($E_{NO+/NO}$ = 0.55 V) showed a much lower value of $k_{ad}$, by five orders of magnitude.[38] Figure 10 shows a plot of ln $k_{ad}$ against $E_{NO^+/NO}$ for the above three complexes. A linear trend can be appreciated, with a *negative slope* of 18.4 ± 0.9 $V^{-1}$ (even though more points should be desirable). This value is in close agreement with the theoretically predicted Marcus-type behavior previously considered for bimolecular reactions occurring with associative character, 19.4 $V^{-1}$. Not unexpectedly, the plot appears as very similar to the one showed in Fig. 5 for the *electrophilic* addition reactions of $[MX_5(NO^+)]^x$ complexes with $OH^-$, although with a *positive slope.*

Six-coordination appears as a necessary condition to achieve autooxidation of bound NO-complexes, on the basis of the apparent *unreactivity* of $[Fe(CN)_4NO]^{2-}$, and also considering similar reactivity patterns found in nonaqueous media for related complexes, namely the non-heme $[Fe(PaPy_3)NO]^+$ complex[22c] and the picket-fence compound [Fe(TpivPP)NO], which reacts with $O_2$ *only* in the presence of pyridine, to give $[Fe(TpivPP)(NO_2)(py)]$.[82]

That the redox potentials of the $MNO^+/MNO^{\bullet}$ couples could predict the NO-autoxidation reactivities appears as quite significant. Some $NO^{\bullet}$-coordination compounds could readily react with $O_2$ in order to provide a fast route to $NO^{\bullet}$-consumption. However, the complexes like $[Fe(CN)_5NO]^{3-}$ could hardly compete with other main sinks for NO, namely its very fast reactions with sGC or with $HbO_2$.[16]

## Reactivity of bound $NO^-$/HNO complexes. Protonation, metal-dissociation and reactions toward electrophiles or nucleophiles

Different methods for preparing HNO-complexes have been described.[39] Protonation of bound $NO^-$ is one of the viable routes to HNO-complexes, as $NO^-$ is expected to be strongly nucleophilic. The recently reported p$K_a$ values for free $^1HNO/^3NO^-$ and $^1HNO/^1NO^-$ are 11.4 and 23, respectively.[39b] However, nothing is known about the p$K_a$ values for *bound* $^1HNO/^1NO^-$ in aqueous solutions. These should be ≥ 10, on the basis of the unchanged electronic and NMR spectra reported for $Mb^{II}HNO$ up to this pH.[41]

In contrast with most of the classical HNO-complexes (Table 1), the solubility in aqueous solution of $Mb^{II}HNO$ is remarkable, as also can be said on the reported inertness toward the release of HNO (hour´s time scale). The latter result has also been observed for $[Fe^{II}(cyclam\text{-}ac)NO]^o$ in acetonitrile.[22a] The inertness of bound $NO^-$/HNO toward dissociation is consistent with the previous postulation of $[Fe(CN)_5HNO]^{3-}$ being a sufficiently long-lived intermediate in the reaction of 1,2-dimethylhydrazine with SNP, eqn. (14),[65] or in the disproportionation reaction of $NH_2OH$ catalyzed by pentacyanoferrates, leading to bound $NO^+$ as one of the oxidized products.[83] HNO has been also proposed as an intermediate in the oxidation of $NH_2OH$ to $NO_2^-$ mediated by the heme-based hydroxylamine oxidoreductase enzyme, HAO.[84]

All the reported HNO-complexes appear as air sensitive, but the products and mechanisms have not been studied in detail.[39] In principle, one would expect a decrease in the nucleophilic reactivity of bound HNO, compared to $NO^-$ complexes. The $[CoL_4NO]$ complexes (formally $Co^{III}NO^-$, with L = diverse tetradentate dianions) react with $O_2$ in nonaqueous media, *only* in the presence of nitrogen- and phosphorus bases (B) to yield the corresponding nitrocompounds, $[CoL_4(NO_2)B]$.[16] The rates of these autoxidation reactions were strongly dependent on the nature of the *trans*-ligand to $NO^-$, thus influencing the nucleophilicity of the $\{CoNO\}^8$ moieties. Other $Ir^{III}NO^-$ complexes are also attacked by $O_2$, although with $NO_3^-$ as products.[16] Systematic kinetic investigations on the autoxidations of $NO^-$/HNO-complexes are in order.

The electrophilic behavior of bound HNO is also biologically relevant, given the known reactivity of free HNO toward the thiolates, rendering $NH_2OH$ and disulfides as products. Recent reactivity studies show that bound HNO reacts under excess NO conditions in the same way as reported for free HNO, eqn. (23), involving formal NO-disproportionation.[85]

$$HNO + 2NO \rightarrow HONO + N_2O \quad (23)$$

## Injecting SNP in the bodily fluids. The fate of NO. Dinitrosyls and disproportionations

It is known that the vasodilation response in mammals occurs readily a few seconds after SNP injection.[18,19] As SNP is thermally very robust, it has been reasonably inferred that a reduction of bound $NO^+$ to NO must be operative, with further release of NO to the medium, in order to activate sGC. The rapid formation of nitrosothiolate-adducts with SNP and their subsequent redox decompositions have been described above through eqns. (16) and (17), respectively. However, the product in (17), $[Fe(CN)_5NO]^{3-}$, is very inert toward NO-dissociation.[43] A second possibility for free NO availability deals with the dissociation of the N(O)SR ligand from $[Fe(CN)_5N(O)SR]^{3-}$. In that case, NO could be generated through the well known catalytic, homolytic decomposition of free N(O)SR's.[86] We also discard in principle such a route because our preliminary measurements indicate that the Fe-N bond dissociation is not sufficiently fast ($k_{-NOSR}$ = *ca.* $10^{-4}$ $s^{-1}$, at 25 ºC).

The rapid vasodilator effect of SNP has been traced to the fast NO-dissociation from $[Fe(CN)_4NO]^{2-}$, formed in eqn. (3).[19] For checking this hypothesis, we were prompted to perform a detailed study of the thermal decomposition of $[Fe(CN)_5NO]^{3-}$ / $[Fe(CN)_4NO]^{2-}$ mixtures, generated through the fast reduction of SNP with dithionite.[87] Scheme 4 includes the reactants, intermediates and products detected in a time scale of hours by using different spectroscopic tools, in the pH range 4-10 and anaerobic medium.

At the left-center of Scheme 4 we show the equilibrium mixture of the reactant complexes, whose decay may be studied independently by UV-vis spectroscopy, by judicious control of pH. At pH 9, the decay of predominant $[Fe(CN)_5NO]^{3-}$ reveals a pseudo-first order decay, with $k_{off}$ =

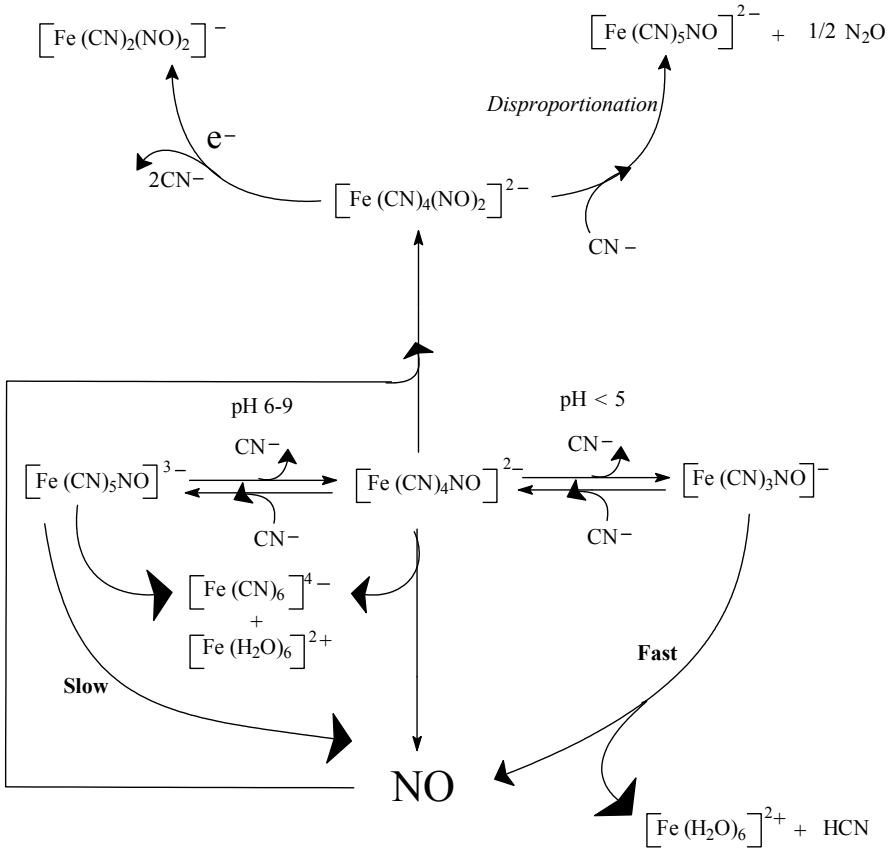


**Scheme 4**

$4 \times 10^{-5}$ $s^{-1}$. This is in fair agreement with the reported value for the dissociation of NO from $[Fe(CN)_5NO]^{3-}$, $k_{-NO}$, (Table 2), considering that some minor $[Fe(CN)_4NO]^{2-}$ is present in the reaction conditions (absence of free cyanide).[73] The formation of NO was detected electrochemically during the first 15 min and was absent after 10 h. The onset of a new band at 2038 $cm^{-1}$, typical of $[Fe(CN)_6]^{4-}$,[73] agrees with eqn. (24), describing a process subsequent to NO-dissociation, involving the successive release and recombination of cyanides.[88] In insufficiently diluted solutions, the products in (24) lead to white precipitates of Prussian Blue type, $Fe_2[Fe(CN)_6].xH_2O$. The formation of inert hexacyano-complexes is probably the reason for the general absence of toxicity in physiological experiments with SNP.

$$[Fe(CN)_5H_2O]^{3-} \rightarrow 5/6[Fe(CN)_6]^{4-} + 1/6Fe^{2+} + H_2O \quad (24)$$

Some $N_2O$ and SNP were observed as minor decomposition products for *ca.* 10 h of reaction.

By working at pH 6, Fig. 11 shows the decay of mixtures containing predominantly $[Fe(CN)_4NO]^{2-}$. The inset includes the absorbance traces at two selected wavelengths fitted to a two-exponential model. A *remarkably slow* monotonic decay at 615 nm (maximum of $[Fe(CN)_4NO]^{2-}$),[52] along with an initial increase and subsequent decrease of an intermediate $I_1$ with maximum at 336 nm can be observed. Values of $k_{obs}$ = 3-6 $\times$ $10^{-5}$ $s^{-1}$ and 1-2 $\times$ $10^{-5}$ $s^{-1}$ were calculated for the steps involving the formation and decay of $I_1$, respectively. From the chronoamperograms, NO was shown to be generated during the first minutes; then, it decreases slowly with time. The formation of $N_2O$ reveals a continuous exponential increase, with $k_{obs}$ = 1.4 $\times$ $10^{-5}$ $s^{-1}$, measured through mass-spectrometry in a pressure-reactor. At the end of the reaction, $[Fe(CN)_6]^{4-}$ was found in low yields, in contrast with free cyanides (60-200%). SNP and $N_2O$ were 40% and 20%, respectively, with respect to the initial concentration of $[Fe(CN)_5NO]^{3-}$. Figure 12a shows the successive IR spectra, with a decreasing intensity of the bands corresponding to $[Fe(CN)_4NO]^{2-}$/$[Fe(CN)_5NO]^{3-}$, along with an increase in the bands for $[Fe(CN)_6]^{4-}$, SNP and $N_2O$. The outstanding feature in Fig. 12a is the appearance of a transient weak absorption at 1695 $cm^{-1}$ (with a maximum intensity attained after 2.5 h), which is absent at the beginning and at the end of the process, revealing its intermediate character. We assign this feature to

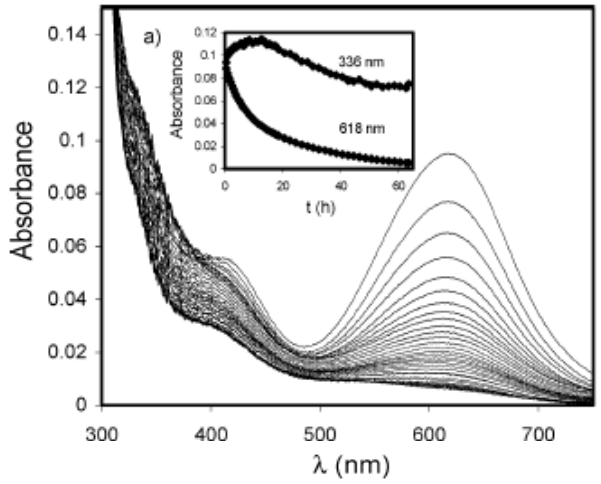


**Figure 11.** Successive UV-vis spectra for the thermal decomposition of predominantly $[Fe(CN)_4NO]^{2-}$, with *ca.* 0.25 mM reduced SNP, pH 6, $T$ = 25.5 ºC, $I$ = 0.1 M. Inset: Kinetic traces at 336 and 618 nm fitted to a double exponential model (SPECFIT).[87]

$\nu_{NO}$ in $I_1$, consistent with the UV-vis results and with isotope-labeling measurements with $^{15}NO$ (downward shift of $\nu_{NO}$, 40 $cm^{-1}$). Figure 12b shows the results of an independent experiment; by adding NO in a controlled way to $[Fe(CN)_4NO]^{2-}$, the IR-peak at 1695 $cm^{-1}$ was reproduced (with a new, weaker one at *ca.* 1737 $cm^{-1}$). Both peaks disappear by adding excess of NO, suggesting that $I_1$ is unstable under these conditions. Finally, the EPR monitoring measurements in Fig. 13 (a) reveals that the initial signal of the reactants´mixture evolves to a different one for a final paramagnetic product (named as $I_2$, see below), with an *EPR-silent intermediate*, also assignable to $I_1$.

We propose that $I_1$ is a *trans*-dinitrosyl species formed after NO-dissociation from $[Fe(CN)_4NO]^{2-}$, eqn. (25), with subsequent coordination to the same complex, eqn. (26):

$$[Fe(CN)_4NO]^{2-} + 2H_2O \rightleftharpoons [Fe(CN)_4(H_2O)_2]^{2-} + NO \quad (25)$$

$$[Fe(CN)_4NO]^{2-} + NO \rightarrow [Fe(CN)_4(NO)_2]^{2-} \quad (26)$$

The EPR-silent properties of $I_1$ can be ascribed to a low-spin Fe(II) center containing two antiferromagnetically coupled NO ligands. Additional support for product identification in (26) is provided by independent UV-vis stopped-flow measurements, showing a first-order rate law in each reactant, with $k_{26} = 4.3 \times 10^4$ $M^{-1}$ $s^{-1}$. Recent reports deal with the coordination of NO to ferrous nitrosyl-porphyrins, giving *trans*-$[Fe(por)(NO)_2]$ in low-temperature solutions.[16] These are also EPR-silent complexes, with similar IR properties as described for $I_1$. From theoretical calculations, a *trans-syn* ($C_{2v}$) conformation has been proposed for $[Fe(TPP)(NO)_2]$. Our preliminary results indicate a similar picture for $[Fe(CN)_4(NO)_2]^{2-}$, which also reproduce the *trans-syn* geometry and provide fairly consistent $\nu_{NO}$ values.

By lowering the pH to 4, the decomposition of $[Fe(CN)_4NO]^{2-}$ becomes faster by two orders of magnitude, with a subsequent release of cyanide, NO and aqueous Fe(II)

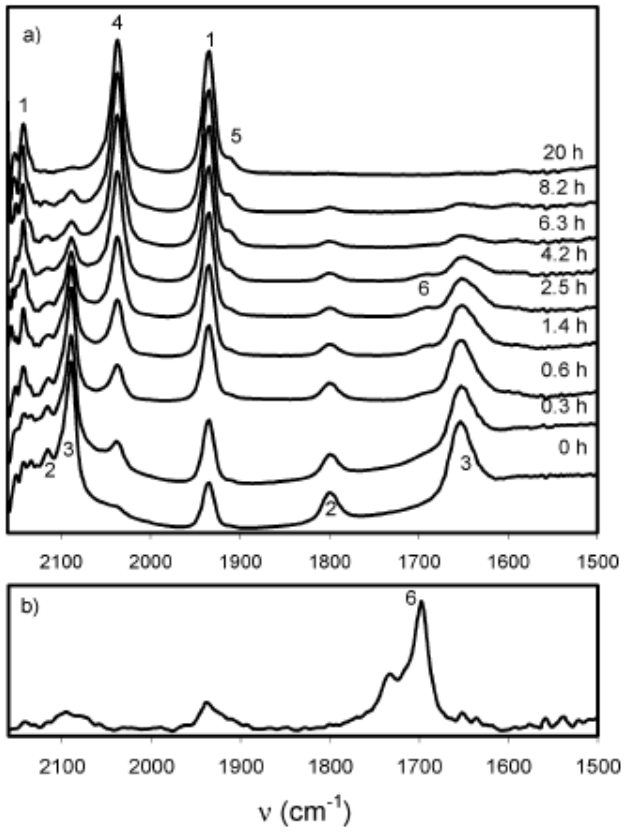


**Figure 12.** (a) IR spectral changes during the thermal decomposition of *ca.* 17 mM reduced SNP, at pH 7, T = 25 ºC, $k_{obs} \approx 5 \times 10^{-5}$ $s^{-1}$ (decay of $\nu_{NO}$). (b) Spectrum obtained after bubbling NO through a 17 mM reduced SNP $D_2O$-solution until first color change. Peak numbers correspond to the following complexes: 1, $[Fe(CN)_5NO]^{2-}$; 2, $[Fe(CN)_4NO]^{2-}$; 3, $[Fe(CN)_5NO]^{3-}$; 4, $[Fe(CN)_6]^{4-}$; 5, $[Fe(CN)_4(OH)NO]^{2-}$; 6, $[Fe(CN)_4(NO)_2]^{2-}$.[87]

ions (right, lower part in Scheme 4). This process is favored by the presence of metal ions (Cu, Fe). Therefore, our final conclusion is that NO requires the previous labilization of more cyanides from $[Fe(CN)_4NO]^{2-}$ in order to be *subsequently* released. We infer that this may occur even under physiological conditions, with local situations (*viz*, near positively charged centers in membranes), favoring complex decomposition through the donor interactions of bound cyanides.[18]

The upper part of Scheme 4 involves a set of reactions comprising the decomposition of $I_1$. As suggested by Figs. 11,12, $I_1$ remains at a low steady-state concentration, suggesting decomposition at a similar rate as its formation (see the $k_{obs}$ values derived from the SPECFIT treatment of UV-vis results). The rigorous 2:1 stoichiometries in SNP:$N_2O$ suggest a disproportionation process, as described by eqns. (27-28):

$$[Fe(CN)_4(NO)_2]^{2-} + CN^- + H^+ \rightarrow [Fe(CN)_5NO]^{2-} + HNO \quad (27)$$

$$2HNO \rightarrow N_2O + H_2O \quad (28)$$

The disproportionation reaction is probably intramolecular for the experiments in the absence of an excess of NO. A

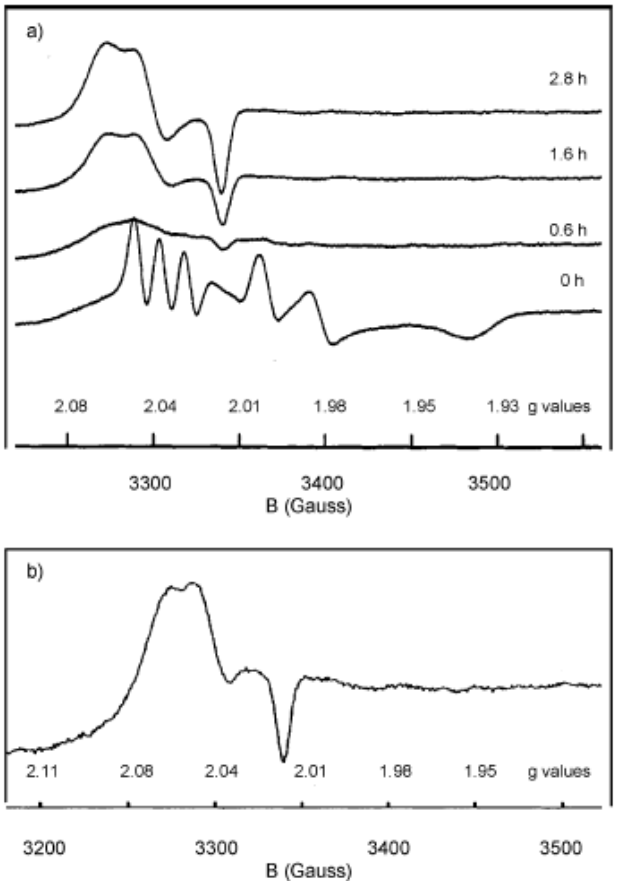


**Figure 13.** (a) EPR spectral changes recorded during the decomposition of a *ca.* 0.26 mM reduced SNP (mixture of tetra- and pentacvano-nitrosyls) at pH 5, $I$ = 0.1 M, T = 25 ºC. (b) Spectrum obtained after bubbling NO through a similar solution.[87]

different path could be present under excess NO, as proposed for related dinitrosyl complexes affording disproportionation.[16]

Finally, Scheme 4 includes an additional, parallel route for the decomposition of $I_1$, as revealed by the EPR properties of the final product at pH 5 (Fig. 13 (b)). We propose that this is also a dinitrosyl species, $I_2$, a new member of the well-characterized series of paramagnetic distorted tetrahedral complexes, $[Fe(L)_2(NO)_2]$, with different L ligands, described as $\{Fe(NO)_2\}^9$. They are known as reversible, labile NO carriers, involved in *trans*-nitrosylation processes.[89] EPR signals assignable to these dinitrosyl complexes have been found in tissue of ascite tumors of mice upon injection with SNP.[90] Some of them, *viz*., with L = thiolates and imidazole, activate sGC to promote vasodilation.[91]

## Conclusions and future directions

We have described an impressive set of reactions afforded by the redox-interconvertible nitrosyl ligands ($NO^+$, $NO^•$, $NO^–$), bound to the pentacyanoferrates (II and III). Similar reactivity patterns might be expected for complexes containing other low-spin $MX_5$ fragments, although with a fine tuning of the structure and reactivity, as described for the nucleophilic and electrophilic additions.

The properties of bound $NO^+$ are generally well understood, though more work is needed with the reduced $NO^•$-complexes. For covering the studies on reactivity, the key point relates to the synthetic efforts needed for obtaining new, well characterized compounds, desirably soluble in aqueous media. Robust $[MX_5NO^•]$ complexes with adequate (quantitative, if possible) control of the *trans*-labilizations would be convenient, with emphasis on M = Fe. With the reactions performed in excess NO-conditions, due account should be paid to possible dinitrosyl formation and/or disproportionation processes, whose systematic study is interesting in its own right, as well as relevant to the enzymatic mechanisms with $NO_2^–$, NO and $N_2O$-reductases.

A special effort should be directed to synthesize and characterize new, water-soluble iron-nitroxyl complexes. Fundamental questions such as $NO^–$ against HNO stability are in order. Redox reactivity of the latter species toward bound or free $NO^•$ are also important.

Once these goals are reached, the future seems promising for significant advances in the research frontier of bound-nitrosyl reactivity toward a variety of biologically relevant substrates.

## Acknowledgments

Support from the University of Buenos Aires, the funding agencies ANPCYT and CONICET, and the VolkswagenStiftung are gratefully acknowledged. The work of collaborators cited below, and particularly that from my previous students, Dr. Federico Roncaroli and Dra. Mariela Videla, are highly appreciated. FR and MV were doctoral fellows, and JAO is a member of the research staff of CONICET.

## References

1 L. Playfair, *Proc. Roy. Soc. (London)*, 1849, **5**, 846.
2 C. C. Johnson, *Arch. Int. Pharmacodyn. Ther*., 1929, **35**, 489.
3 P. P. Moracca, E. M. Bilte, D. E. Hale, C. E. Wasmuth and E. F. Pontasse, *Anesthesiology*, 1962, **23**, 193.
4 M. Feelisch and J. S. Stamler, eds. *Methods in Nitric Oxide Research*, John Wiley and Sons: Chichester, England, 1996.
5 F. C. Fang, ed. *Nitric Oxide and Infection*, Kluwer Academic/Plenum Publishers: New York, 1999.
6 L. J. Ignarro, ed. *Nitric Oxide, Biology and Pathobiology*; Academic Press: San Diego, CA, 2000.
7 (a) G. B. Richter-Addo and P. Legdzins, *Metal Nitrosyls*; Oxford University Press: New York, 1992. (b) J. A. McCleverty, *Chem. Rev*., 2004, **104**, 403.
8 J. A. Olabe and L. D. Slep, in *Comprehensive Coordination Chemistry II, from Biology to Nanotechnology*; ed. J. A. Mc Cleverty and T. J. Meyer, Elsevier, Oxford, 2004; Vol. 1, p 603.
9 L. Cheng and G. B. Richter-Addo, in *The Porphyrin Handbook*, Vol. 4, Ch.33, eds. K. M. Kadish, K. M. Smith and R. Guilard, Academic Press: New York, 2000.
10 (a) W. R. Scheidt and M. K. Ellison, *Acc. Chem. Res*., 1999, **32**, 350. (b) G. R. A. Wyllie and W. R. Scheidt, *Chem. Rev*., 2002, **102**, 1067.
11 M. Hoshino, L. Laverman and P. C. Ford, *Coord. Chem. Rev.,* 1999, **187**, 75.
12. A. Franke, F. Roncaroli and R. van Eldik, *Eur. J. Inorg. Chem*., 2007, 773, and references therein.
13 J. A. Olabe, *Adv. Inorg. Chem.*, 2004, **55**, 61.
14 L. M. Baraldo, P. Forlano, A. R. Parise, L. D. Slep and J. A. Olabe, *Coord. Chem. Rev.*, 2001, **219-221**, 881.

15 (a) B. L. Westcott and J. H. Enemark, in *Inorganic Electronic Structure and Spectroscopy*; eds. E. I. Solomon and A. B. P. Lever, Wiley, New York, 1999; Vol. II, p 403. (b) R. D. Feltham and J. H. Enemark, *Top. Inorg. Organomet. Stereochem*., 1981, **12**, 155. (c) J. H. Enemark and R. D. Feltham, *Coord. Chem. Rev.*, 1974, **13**, 339.

16 (a) P. C. Ford, L. E. Laverman and I. M. Lorkovic, *Adv. Inorg. Chem*., 2003, **54**, 203. (b) P. C. Ford and I. M. Lorkovic, *Chem. Rev.*, 2002, **102**, 993. (c) P. C. Ford, B. O Fernandez and M. D. Lim, *Chem. Rev*. 2005, **105**, 2439.

17 F. Roncaroli, M. Videla, L. D. Slep and J. A. Olabe, *Coord. Chem. Rev*., 2007, **251**, 1903.

18 F. Bottomley, in *Reactions of Coordinated Ligands,* ed. P. S. Braterman, Plenum Publishing Corp., New York, 1989, Vol. 2.

19 A. R. Butler and I. L. Megson, *Chem. Rev.*, 2002, **102**, 1155.

20 M. J. Clarke and J. B. Gaul, *Struct. Bonding (Berlin)*, 1993, **81**, 147.

21 J. S. Stamler, D. J. Singel and J. Loscalzo, *Science*, 1992, **258**, 1898.

22 (a) R. G. Serres, C. A. Grapperhaus, E. Bothe, E. Bill, T. Weyhermuller, F. Neese and K. Wieghardt, *J. Am. Chem. Soc.*, 2004, **126**, 5138. (b) D. Sellmann, N. Blum, F. W. Heinemann and B. A. Hess, *Chem. Eur. J*., 2001, **7**, 1874. (c) R. K. Afshar, A. K. Patra, E. Bill, M. M. Olmstead and P. K. Mascharak, *Inorg. Chem*., 2006, **45**, 3774. (d) M. K. Ellison, C. E. Schultz and W. R. Scheidt, *Inorg. Chem*., 1999, **38**, 100. (e) M. D. Carducci, M. R. Pressprich and P. Coppens, *J. Am Chem. Soc*., 1997, **119**, 2669. (f) J. A. Olabe, L. A. Gentil, G. E. Rigotti and A. Navaza, *Inorg. Chem.*, 1984, **23**, 4297. (g) L. M. Baraldo, M. S. Bessega, G. E. Rigotti and J. A. Olabe, *Inorg. Chem.*, 1994, **33**, 5890. (i) P. Gans, A. Sabatini and L. Sacconi, *Inorg. Chem*., 1966, **5**, 1877. (i) P. Singh, B. Sarkar, M. Sieger, M. Niemeyer, J. Fiedler, S. Zalis and W. Kaim, *Inorg. Chem*., 2006, **45**, 4602. (j) F. Bottomley, S. G. Clarkson and S. B. Tong, *J. Chem. Soc., Dalton Trans*., 1974, 2344. (k) F. Di Salvo, N. Escola, D. A. Scherlis, D. A. Estrin, C. Bondia, D. Murgida, J. M. Ramallo-López, F. G. Requejo, L. Shimon and F. Doctorovich, *Chem. Eur. J.*, 2007, **12**, 8428.

23 (a) H. Nasri, M. K. Ellison, S. Chen, B. H. Huynh and W. R. Scheidt, *J. Am. Chem. Soc*., 1997, **119**, 6274. (b) R. Nast and J. Schmidt, *Angew. Chem. Int. Ed. Engl*., 1969, **8**, 383. (c) K. Pohl, K. Wieghardt, B. Nuber and J. Weiss, *J. Chem. Soc., Dalton Trans.,* 1987, 187. (d) C. A. Brown, M. A. Pavlovsky, T. E. Westre, Y. Zhang, B. Hedman, K. O. Hodgson and E. I. Solomon, *J. Am. Chem. Soc*., 1995, **117**, 715. (e) M. Li, D. Bonnet, E. Bill, F. Neese, T. Weyhermuller, N. Blum, D. Sellmann, and K. Wieghardt, *Inorg. Chem*., 2002, **41**, 3444.

24 (a) M. González Lebrero, D. A. Scherlis, G. L. Estiú, J. A. Olabe and D. A. Estrin, *Inorg. Chem*., 2001, **40**, 4127. (b) D. A. Snyder and D. L. Weaver, *Inorg. Chem*., 1970, **9**, 2760. (c) D. Sellmann, T. Gottschalk-Gaudig, D. Haussinger, F. W. Heinemann and B. A. Hess, *Chem. Eur. J*., 2001, **7**, 2099. (d R. D. Wilson and J. A. Ibers, *Inorg. Chem.*, 1979, **18**, 336. (e) R. Melenkivitz and G. L. Hillhouse, *Chem. Commun*., 2002, 660.

25 D. M. Mingos, *Inorg. Chem*., 1973, **12**, 1209.

26 (a) P. T. Manoharan and H. B. Gray, *J. Am. Chem. Soc*., 1965, **87**, 3340. (b) R. F. Fenske and R. L. DeKock, *Inorg. Chem*., 1972, **11**, 437.

27 F. A. Walker, *J. Inorg. Biochem*., 2005, **99**, 216.

28 S. K. Wolfe and J. H. Swinehart, *Inorg. Chem*., 1975, **14**, 1049.

29 (a) E. Tfouni, M. Krieger, B. R. McGarvey and D. W. Franco, *Coord. Chem. Rev*., 2003, **236**, 57. (b) M. Videla, S. E. Braslavsky and J. A. Olabe, *Photochem. Photobiol. Sci.*, 2005, **4**, 75. (c) R. Prakash, A. U. Czaja, F. W. Heinemann, D. Sellmann, *J. Am. Chem. Soc*., 2005, **127**, 13758. (d) F. de Souza Oliveira, V. Togniolo, A. C. Tedesco, and R. Santana da Silva, *Inorg. Chem. Commun.*, 2004, **7**, 160.

30 (a) P. Gütlich, Y. Garcia and Th. Woike, *Coord. Chem. Rev*., 2001, **219-221**, 839. (b) V. Rusanov, Sv. Stankov and A. X. Trautwein, *Hyperfine Interactions,* 2002, **144/145**, 307.

31 P. Coppens, I. Novozhilova and A. Kovalevsky, *Chem. Rev*., 2002, **102**, 861.

32 M. E. Chacón Villalba, J. A.Güida, E. L. Varetti and P. J. Aymonino, *Inorg. Chem*., 2003, **42**, 2622, and references therein.

33 (a) P. Boulet, M. Buchs, H. Chermette, C. Daul, F. Gilardoni, F. Rogemond, C. W. Schlapfer and J. Weber, *J. Phys. Chem. A,* 2001, **105**, 8991. (b) S. I. Gorelsky and A. B. B. Lever, *Int. J. Quantum Chem*., 2000, **80**, 636.

34 D. Schaniel, Th. Woike, C. Merschjann and M. Imlau, *Phys. Rev. B,* 2005, **72**, 195119.

35 (a) J. A. Güida, O. E. Piro, P. S. Shaiquevich and P. J. Aymonino, *Solid State Commun*., 1997, **101**, 471. (b) J. A. Guida, O. E. Piro and P. J. Aymonino, *Inorg. Chem*., 1995, **34**, 4113.

36 (a) M. Wanner, T. Scheiring, W. Kaim, L. D. Slep, L. M. Baraldo, J. A. Olabe, S. Zalis and E. J. Baerends, *Inorg. Chem.*, 2001, **40**, 5704. (b) J. D. W. van Voorst and P. Hemmerich, *J. Chem. Phys*., 1966, **45**, 3914.

37 S. Frantz, B. Sarkar, M. Sieger, W. Kaim, F. Roncaroli, J. A. Olabe and S. Zalis, *Eur. J. Inorg. Chem*., 2004, 2902.

38 M. Videla, J. S. Jacinto, R. Baggio, M. T. Garland, P. Singh, W. Kaim, L. D. Slep and J. A. Olabe, *Inorg. Chem*., 2006, **45**, 8608.

39 (a) P. J. Farmer and F. Sulc, *J. Inorg. Biochem.* 2005, **99**, 166. (b) K. M. Miranda, *Coord. Chem. Rev*., 2005, **249**, 433 and references therein.

40. L. Hannibal, C. A. Smith, D. W. Jacobsen and N. E. Brasch, *Angew. Chem. Int. Ed*., 2007, **46**, 5140.

41 (a) R. Lin and P. J. Farmer, *J. Am. Chem. Soc*., 2000, **122**, 2393. (b) C. E. Immoos, F. Sulc, P. J. Farmer, K. Czarnecki, D. Bocian, A. Levina, J. B. Aitken, R. Armstrong and P. A. Lay, *J. Am. Chem. Soc*., 2005, **127**, 814.

42 (a) J. Masek and E. Maslova, *Coll. Czech. Chem. Commun*., 1974, **39**, 2141. (b) A. Montenegro, S. E. Bari, D. Murgida, L. D. Slep and J. A. Olabe, work in progress.

43 F. Roncaroli, J. A. Olabe and R. van Eldik, *Inorg. Chem.*, 2003, **42**, 4179.

44 A. Wanat, T. Schneppensieper, G. Stochel, R. van Eldik, E. Bill and K. Wieghardt, *Inorg. Chem*., 2002, **41**, 4.

45 T. Schneppensieper, A. Wanat, G. Stochel and R. van Eldik, *Inorg. Chem.*, 2002, **41**, 2565.

46 L. E. Laverman and P. C. Ford, *J. Am. Chem. Soc*., 2001, **123**, 11614.

47 M. Wolak and R. van Eldik, R. *J. Am. Chem. Soc*., 2005, **127**, 13312.

48 F. Roncaroli, J. A. Olabe and R. van Eldik, *Inorg. Chem.*, 2002, **41**, 5417.

49 A. Czap and R. van Eldik, *Dalton Trans*., 2003, 665.

50 P. C. Ford and L. E. Laverman, *Coord. Chem. Rev.*, 2005, **249**, 391.

51 (a) H. E. Toma, N. M. Moroi and N. Y. M. Iha, *An Acad. Brasil. Cienc*., 1982, **54**, 315. (b) M. I. Finston and H. G. Drickamer, *J. Phys. Chem*., 1981, **85**, 50. (c) J. Legros, *J. Chim. Phys. Phys.-Chim. Biol*., 1964, **61**, 909. (d) H. E. Toma, J. M. Malin and E. Giesbrecht, *Inorg. Chem*., 1973, **12**, 2084. (e) H. E. Toma and J. M. Malin, *Inorg. Chem*., 1973, **12**, 2080. (f) H. E. Toma, A. A. Batista and H. B. Gray, *J. Am. Chem. Soc*., 1982, **104**, 7509. (g) I. Maciejowska, R. van Eldik, G. Stochel and Z. Stasicka, *Inorg. Chem*., 1997, **36**, 5409.

52 R. P. Cheney, M. G. Simic, M. Z. Hoffman, I. A. Taub and K. D. Asmus, *Inorg. Chem*., 1977, **16**, 2187.

53 (a) A. D. James and R. S. Murray, *J. Chem. Soc., Dalton Trans*., 1977, 326. (b) Stochel, G. and R. van Eldik, *Inorg. Chim. Acta*, 1991, **190**, 55.

54 J. N. Armor and S. D. Pell, *J. Am. Chem. Soc*., 1973, **95**, 7625.

55 R. van Eldik, *Coord. Chem. Rev*., 2007, **251**, 1649, and references therein.

56 J. H. Swinehart and P. A. Rock, *Inorg. Chem*., 1966, **5**, 573.

57 A. A. Chevalier, L. A. Gentil and J. A. Olabe, *J. Chem. Soc., Dalton Trans*., 1991, 1959.

58 F. Roncaroli, M. E. Ruggiero, D. W. Franco, G. L. Estiu and J. A. Olabe, *Inorg. Chem.*, 2002, **41**, 5760.

59 R. A. Marcus, *J. Phys. Chem.*, 1968, **72**, 891.

60 E. Jee, S. Eigler, N. Jux, A. Zahl and R. van Eldik, *Inorg. Chem.*, 2007, **46**, 3336.

61 J. A. Olabe and G. L. Estiú, *Inorg. Chem*., 2003, **42**, 4873.

62 (a) N. E. Katz, M. A. Blesa, J. A. Olabe and P. J. Aymonino, *J. inorg. nucl. Chem*., 1980, **42**, 581. (b) I. Maciejowska, Z. Stasicka, G. Stochel and R. van Eldik, *J. Chem. Soc., Dalton Trans*., 1999, 3643.

63 L. Dozsa, V. Kormos and M. T. Beck, *Inorg. Chim. Acta*, 1984, **82**, 69.

64 S. K. Wolfe, C. Andrade and J. H. Swinehart, *Inorg. Chem*., 1974, **13**, 2567.

65 M. M. Gutiérrez, V. T. Amorebieta, G. L. Estiú and J. A. Olabe, *J. Am. Chem. Soc*., 2002, **124**, 10307.
66 F. Doctorovich and F. Di Salvo, *Acc. Chem. Res.*, 2007, **40**, 985.
67 I. M. Wasser, S. de Vries, P. Moënne-Loccoz, I. Schröder and K. D. Karlin, *Chem. Rev*., 2002, **102**, 1201.
68 B. O. Fernandez and P. C. Ford, *J. Am. Chem. Soc*., 2003, **125***,* 10510.
69 S. Goldstein and G. Czapski, *J. Am. Chem. Soc.*, 1995, **117**, 12078.
70 J. E. Jee and R. van Eldik, *Inorg. Chem.*, 2006, **45**, 6523.
71 M. J. Akhtar, F. T. Bonner, A. Borer, I. Cooke and M. N. Hughes, *Inorg. Chem*., 1987, **26**, 4379.
72 M. D. Johnson and R. G. Wilkins, *Inorg. Chem.*, 1984, **23**, 231.
73 J. D. Schwane and M. T. Ashby, *J. Am. Chem. Soc*., 2002, **124**, 6822.
74 L. L. Perissinotti, D. A. Estrin, G. Leitus and F. Doctorovich, *J. Am. Chem. Soc.*,, 2006, **128**, 2512.
75 (a) P. Morando, E. B. Borghi, L. M. Schteingart and M. A. Blesa, *J. Chem. Soc., Dalton Trans*., 1981, 435. (b) K. Szacilowski, G. Stochel, Z. Stasicka and H. Kisch, *New J. Chem*., 1997, **21**, 893.
76 K. Szacilowski, A. Wanat, A. Barbieri, E. Wasiliewska, M. Witko, G. Stochel and Z. Stasicka, *New J. Chem.*, 2002, **26**, 1495.
77 F. Roncaroli and J. A. Olabe, *Inorg. Chem*., 2005, **14**, 4719.
78 (a) P. A. Rock and J. H. Swinehart, *Inorg. Chem*., 1966, **5**, 1078. (b) C. Andrade and J. H. Swinehart, *Inorg. Chem*., 1972, **11**, 648.
79 J. K. S. Moller and L. H. Skibsted, *Chem. Eur. J*., 2004, **10**, 2291.
80 M. Videla, F. Roncaroli, L. D. Slep and J. A. Olabe, *J. Am. Chem. Soc.*, 2007, **129**, 278, and references therein.
81 J. N. Armor and M. Z. Hoffman, *Inorg. Chem.*, 1975, **23**, 231.
82 L. Cheng, D. R. Powell, M. A. Khan and G. B. Richter-Addo, *Chem. Commun*., 2000, 2301.
83 G. Alluisetti, A. E.Almaraz, V. T. Amorebieta, F. Doctorovich and J. A. Olabe, *J. Am. Chem. Soc*., 2004, **126**, 13432.
84 O. Einsle, A. Messerschmidt, R. Huber, P. M. H. Kroneck and F. Neese, *J. Am. Chem. Soc.*, 2002, **124**, 11737.
85 A. V. Marchenko, A. N. Vedernikov, D. F. Dye, M. Pink, J. M. Zaleski and K. G. Caulton, *Inorg. Chem*., 2002, **41**, 4087.
86 J. S. Stamler and E. J. Toone, *Curr. Op. Chem. Biol*., 2002, **6**, 779.
87 F. Roncaroli, R. van Eldik and J. A. Olabe, *Inorg. Chem.*, 2005, **44**, 2781.
88 J. A. Olabe and H. O. Zerga, *Inorg. Chem*., 1983, **22**, 4156.
89 T. Ueno, Y. Suzuki, S. Fujii, A. F. Vanin and T. Yoshimura, *Biochem. Pharmacol*., 2002, **63**, 485.
90 L. Burlamaschi, G. Martin and E. Tiezzi, *Inorg. Chem*., 1969, **8**, 2021.
91 A. F. Vanin, R. A. Stukan, E. B. Mabuchkina, *Biochim. Biophys. Acta*, 1996, **1295**, 5.

 

*José A. Olabe was born in San Sebastián (Spain) and carried out his studies in Argentina. He obtained his PhD at the University of La Plata (1968), and undertook post-doctoral work at the same University. He was a Visiting Professor at SUNY Stony Brook (NY), working with Prof. Albert Haim (1989). As a Professor of Inorganic and Physical Chemistry, he joined the Universities of Luján, Mar del Plata, and Buenos Aires (1986-), and is a member of CONICET, the national research council in Argentina. Since 2007, he is a Consulting Professor at the Facultad de Ciencias Exactas y Naturales, University of Buenos Aires. His research interest deals with the coordination chemistry of small nitrogenated molecules, with emphasis in kinetic and mechanistic studies.*